Deanship of Graduate Studies

Al-Quds University

Spectroscopic Approach of Protein- Androgen Complexes:

Study of Testosterone Interactions with Human Serum Albumin "HSA"

Rawan Mohammad Khaled Qawasmeh

M.Sc.Thesis

Jerusalem-Palestine

1436/2014

Spectroscopic Approach of Protein- Androgen Complexes:

Study of Testosterone Interactions with Human Serum Albumin "HSA"

Prepared by:

Rawan Mohammad Khaled Qawasmi

Supervisors:

Dr. Musa Abu-Teir

Prof. Mahmoud Abu-hadid

A thesis submitted in partial fulfillment of requirements for the degree of master of physics department- Al-Quds University

1436/2014

Al-Quds University

Deanship of Graduate Studies

Physics Department

Thesis Approval

Spectroscopic Approach of Protein- Androgen: Study of Testosterone Interaction with Human Serum Albumin "HSA"

Prepared by: Rawan Mohammad Khaled Qawasmi

Registration No.: 21112760

Supervisors: Dr. Musa Abu-Teir

Prof. Mahmoud Abu-hadid

Master thesis submitted and accepted, Date: / / 2014

The names and signatures of the examining committee members as follows:

1- **Head of Committee: ……... Signature ……**
2- **Internal Examiner: ……. Signature ……**
3- **External Examiner: …… Signature ……..…..**

Jerusalem-Palestine

1436/ 2014

Dedication

I dedicate this work to my family. A special feeling of gratitude to my lovely parents whose words of encouragement and push for tenacity ring in my ears. My beloved four sisters have never left my side and never stopped pushing me forward. Not just this work but my heart is dedicated for them. A special dedication for my brother and his funny spirit.

I also dedicate this work to many special friends in my life who always support me and gave me the identity for being who I am. Special dedications to my teachers, I will always appreciate every nice and encouraging word have been said to me by my teachers for my entire life.

I also dedicate my work to my colleagues either in my educational or career stages in my life. I do appreciate their support by my heart.

I dedicate this work for everyone respected my attitude and believed in me and great thanks for everyone who was and still is special for me in any stage of my life.

I love you all.

Rawan Mohammad Khaled Qawasmi

Declaration:

I certify that this thesis submitted for the degree of master is the result of my own research, except where otherwise acknowledged, and that this thesis (or any part of the same) has not been submitted for a higher degree to any other university or institution.

Signed:

Rawan Mohammad Khaled Qawasmi.

Date: / /

Acknowledgments

Always the first and last great thanks is to Allah, who gave me the ability and energy to accomplish this work, all this will hove not happen without his blessing. Thanks to Allah for all his graces upon us.

Great thanks for everyone who have taught me a word during my educational. Thanks for being generous with your expertise and precious time.

My great thanks to my supervisors. First of all, Prof. Mahmoud Abu-hadid who has made me all the time motivated and curious about knowing and kept me working. Thank you for your precious help not just in Biological field. Prof. Abu-hadid supported me a lot during the research in experimental steps, impressive knowledge, ability of analysis and deep discussion, positive criticism and his impressive computer skills. Thank you for being my supervisor.

My great thanks also is for my dear Supervisor Dr. Musa Abu-Teir for every moment he gave to me from his precious time, for his permanent support, encouragement, physical knowledge, experimental instructions, and his positive energy all the time. Thank you for being so supportive to me.

I would like to thank all my teachers in physics department in Al-Quds University and Polytechnic University. Special thanks to all my master courses teachers. Thank you for every knowledge and support you gave to me.

Great thanks to every technician in Al-Quds University helped me in my experimental work. Thanks to Mr. Sameh Nusiabe, Ms. Mariam Faroun and Ms. Leena Qawasmeh.

Special thanks to my job colleagues and my manager for being so supportive and understanding. My endless thanks are to my family for their love and belief in me.

Abstract

The molecular interactions between HSA and Testosterone have been successfully investigated. The absorption, distribution and metabolism of many molecules can be altered based on their affinity to HSA. HSA is often increases the apparent solubility of hydrophobic ligands in plasma and modulate their delivery to cells. In this study, the interaction between Testosterone and HSA has been investigated using UV-VIS absorption spectrophotometry and FT-IR spectroscopy; binding constant and the effects on the protein secondary structure have been confirmed. From UV-VIS absorption spectrophotometry which showed an increase in the absorption intensity with increasing the molecular ratios of testosterone to HSA, it is found that the value of the binding constant of testosterone to HSA, K equals $34.9\times102\ M^{-1}$. FT-IR spectroscopy in the mid infrared region with Fourier self deconvolution, second derivative, difference spectra, peak picking and curve fitting were used to determine the effect of Testosterone on the protein secondary structure in the amides I, II and III regions. From the FTIR absorbance spectra, it is found that the intensity of the absorption bands increased with increasing the molecular ratios of Testosterone, where from the deconvoluted and curve fitted spectra, it is found that the absorbance intensity for α- helices decreases relative to β- sheets; this decrease in intensity is related to the formation of H- bonding in the complex molecules.

Table of content

List of tables:

List of Figures

List of symbols:

Symbol	Description
Δ	Un-saturation site
K	Binding constant
λ	Wavelength
H	Planck's constant
N	Frequency
E_{total}	Total energy
E_{ele}	Electronic energy
E_{vib}	Vibrational energy
E_{rot}	Rotational energy
m_A, m_B	Mass of particles A,B
Δx	Displacement of the spheres along the x-axis from equilibrium position
F_x	Restoring force acts on the spheres
Ƒ	The spring or force constant
V	The potential energy
T	The kinetic energy of the oscillating motion
μ	The reduced mass
Δx`	Velocity
Ω	Circular frequency of the harmonic vibration
C	Speed of light
Ѵ	Circular frequency in wave-numbers
E_v	The potential energy for harmonic oscillator approximation
V	Vibrational level
A	Constant for a particular molecule.

D_{eq}	The dissociation energy.
w_e	Oscillating frequency
$\hat{w}_e$	Oscillation frequency in wave number
X_e	The an-harmonicity constant
R	Inter-nuclear separation
E_o (v)	The maximum amplitude of the beam at z=0
I_0	The radiant power incident on the sample
$I(z_1, z_2, v)$ dv	The intensity after recombination of the beams for the fixed spectral range dv
S(v)	The spectrum
A_0	The initial absorption of protein at 280 nm in the absence of ligand
A_∞	The final absorption of the ligated protein
A	The recorded absorption at different Testosterone concentrations (L).
S_0	The ground singlet electronic state
S_1 and S_2	The successively higher energy excited singlet electronic states
T_1	The lowest energy triplet state
$h\upsilon_{EM}$	Energy of photon emitted
$h\upsilon_{EX}$	The excitation photon energy
K	The Stern-Volmer quenching constant
k_q	The bimolecular quenching constant
T	The unquenched lifetime
[Q]	The quencher concentration.
F_0	Fluorescence intensity without quencher
F	Fluorescence intensity with quencher
K_{sv}	The Stern-Volmer quenching constant
L	The quencher concentration
B	The path length
A	The absorptivity

List of used abbreviations:

Abbreviation	Representation
HSA	Human Serum Albumin
pH	Power of hydrogen
UV-VIS	Ultraviolet –visible light
FT-IR	Fourier Transform Infra-red
MRI	Magnetic resonance image
CAT	Computer assisted tomography scanning
PET	Positron Emission Tomography
IR	Infra-red
FSD	Fourier self deconvolution
EM	Electromagnetic
Mid-IR	Middle infrared
T	Transmittance
A	Absorbance
C	Concentration
Nm	Nanometer
LED’s	Light emitting diodes
ICT	Intra-molecular charge transfer
Diff	Difference

Chapter One

Introduction

Chapter one

Introduction

Hormones are the most familiar to the general public, due probably to the widespread pharmacological use and abuse of steroid hormones for diverse purposes, such as contraception and body building (Hardie, 1991). Steroids hormones mainly can act as a chemical messenger in a wide range of species and target tissues to produce both slow genomic responses and rapid non-genomic responses (Norman et al. 2004). They have many physiological effects on human body; their incorrect concentration may cause abnormalities in human body (Abu Teir et al. 2010). Steroid hormones help control metabolism, inflammation, immune functions, salt and water balance, development of sexual characteristics and the ability to withstand illness and injury (Frye, CA 2009).

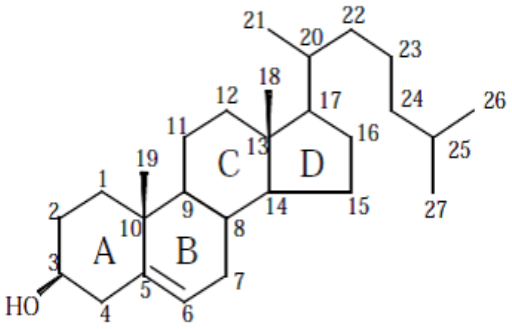

Figure 1.1: Chemical Structure of cholesterol (Norman et al 2004).

In human all steroid hormones are derived from cholesterol and differ only in the ring structure and side chains attached to it (Brandt 1999). Since cholesterol is a non-polar and hydrophobic molecule steroid hormones are insoluble in water but lipid soluble and they have to be carried in the blood bound to specific carrier proteins such as sex hormone-binding globulin or corticosteroid-binding globulin. Sex steroid binding globulin carries testosterone and estradiol (Frye, CA 2009).

Testosterone is a steroid hormone from the androgen group which is found in males and in smaller amount in female. It is 7-8 times concentrated in human males' plasma than in human females. The metabolic consumption of testosterone in males is greater. Testosterone is classified as a strong androgen and secreted primarily from the testicles of males and the ovaries of females, while small amounts of testosterone and weak androgens such as anabolic steroids are secreted by the adrenal gland (Reed WL et al 2006).

The chemical structure of testosterone is ($C_{19}H_{28}O_2$) (Brandt, 1999). It is classified as Δ4 steroid as the double bond (un-saturation site) is located at 4-5 position. Testosterone chemical structure lacks the 2-carbon side-chain attached to the 17th position existed in the cholesterol structure, making it a 19-carbon steroid. In addition the side-chain is replaced by a 17β-hydroxyl (Brandt 1999).

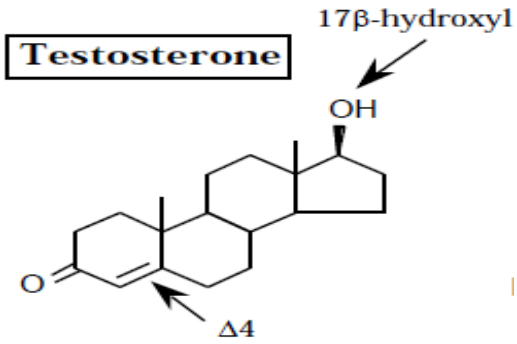

Figure 1.2: The chemical structure of testosterone (Frye CA 2009).

Human serum albumin HSA is an abundant plasma protein that binds a wide variety of hydrophobic ligands including fatty acids, bilirubin, thyroxin and hemin and drugs (Carter et al. 1989; Abu Teir et al. 2010). The most important physiological role of the protein is to bring such solutes into blood stream and then deliver them to the target organs, as well as to maintain the PH and osmotic pressure of plasma (Norman A.W et al. 2004). HSA concentration in human plasma is 40 mg/ml (Tushar et al. 2008). Its structure and function will be discussed briefly in chapter two.

The molecular interactions between HSA and some compounds have been investigated successfully (Gudrum et al. 2002; Ouameur et al. 2004; Ji-Sook et al. 2006; Abu Teir et al. 2010; Abu Teir et al. 2014; Darwish et al. 2010). It has recently been proved that serum albumin plays a decisive role in the transport and disposition of variety of endogenous and exogenous compound such as fatty acids, hormones, bilirubin, drugs (Tang et al. 2006).

The distribution and metabolism of many biologically active compounds in our body whether drugs or natural products are correlated with their affinities toward serum albumin which is the most abundant protein carrier in our plasma. The study of the interaction of such molecules for example testosterone with albumin is of a fundamental importance.

Some investigations have been applied on Testosterone-HSA interaction but none determined in details either Testosterone-HSA binding constant (k) or the effect of testosterone complexes on the protein structure. Some investigations only indicated that the interaction occurred and others used the equilibrium dialysis method to calculate the binding constant k (Pearlman, H. W. 1967; Litwack. G. 1970).

Infrared spectroscopy provides measurements of molecular vibrations due to the specific absorption of infrared radiation by chemical bonds. It is known that the form and frequency of the Amide I band, which is assigned to the C=O stretching vibration within the peptide bonds is very characteristic for the structure of the studied protein. From the band secondary structure, components peaks (α-helix, β-strand) can be derived and the analysis of this single band allows elucidation of conformational changes with high sensitivity (Darwish et al. 2010).

For the IR our work was limited to the mid-range, which covers the wave number range from 4000 to 400 cm^{-1}. This range includes bands that arise from three conformational sensitive vibrations within the peptide backbone (Amides I, II and III) of these vibrations. Amide I is the most widely used and can provide information on the secondary structure composition and structural stability (Cui, A et al.2008; Kang, J et al. 2004; Rondeau, P.A et al. 2007; Abu Teir et al. 2010). Other spectroscopy techniques are usually used in studying the interaction of drugs and proteins. Fluorescence and UV spectroscopy are commonly used because of their high sensitivity, rapidity and ease of implementation. (Wybranowski, T et al. 2008; Li, J et al. 2008; Li,Y et al. 2006).

In addition we have conducted an experimental investigation of the effects of the interaction of the male hormone (testosterone) with HSA by means of UV-VIS spectrophotometer, fluorescence spectrophotometer, and FT-IR spectroscopy in addition to that it is a comparison between cholesterol-HSA, progesterone-HSA and testosterone-HSA bindings.

This thesis is made of five chapters: chapter two discusses the theoretical aspects to guide readers to the important ideas of this study. Chapter three includes details of the experimental, procedures, and instruments used. In chapter four the results obtained are presented and discussed. Chapter five summarizes the conclusions and future work.

Chapter Two

Theoretical Background

Chapter Two

Theoretical Background

Biophysics represents a bridge between biology and physics. The research concentrates on issues related to medicine such as monitoring of heart and brain functions. Biophysicists invented instruments for detecting, purifying, imaging, and manipulating chemicals and materials. Biophysics contributes to the development of medical imaging technologies including magnetic resonance image (MRI), computer assisted tomography scanning (CAT), PET scans, Fourier transform (FT-IR), UV-VIS and fluorescence spectrophotometers. Advanced biophysical research instruments are the daily workhorses of drug development in the world's pharmaceutical and biotechnology industries. Spectrophotometers are powerful tools for studying biological samples such as proteins.

This chapter will cover the theoretical aspects of our work. The first section includes a short historical background about the development of FT-IR spectroscopy and electromagnetic spectrum. Section two covers briefly molecular vibrations, and the following three sections discuss the spectroscopic approaches used in this work; FT-IR, UV-VIS, and fluorescence spectrophotometers. The last section reviews protein structures and we used the model "Human Serum Albumin (HSA)".

2.1 Fourier Transform Infrared (FT-IR) development.

FT-IR spectroscopy has been used to study the secondary structure composition, structural dynamics, conformational changes (effects of ligand binding, temperature, pH and pressure), structural stability and aggregation of proteins. Such information can be deduced from the spectral parameters: band position, band width and absorption.

The high standing is due to the sensitivity and stability of spectrophotometers that are valuable tools for the investigation of protein structural changes during molecular interactions (Kong, J et al. 2007). IR spectroscopy is one of the most common spectroscopic techniques used for structure determination in biological systems, due to the high content of an IR spectrum and sensitivity to the chemical composition of molecules. (Uversky et al. 2007).

The discovery of infrared electromagnetic waves is dated back to the 19th century. Sir William Herschel was the first to recognize their existence in 1800. Since then, scientists have established various ways to utilize them. During 1882-1900 several investigations were made into the IR region.

Because of the numerical complexities of the Fourier procedure, it was until 1949 when Peter Fellgett calculated a spectrum from an interferogram. In 1964 the discovery of the fast Fourier transform (FTT) algorithm by James Cooley and John Tukey reduced the time for the computer calculation of the transform from hours to just few seconds and spectacular advances have been made in the instrumentation from single beam to double beam dispersive spectrometers (Derrick, M.R et al. 1999).

Lakowicz, 2006 reported the development of a number of mathematical techniques, such as Fourier self deconvolution (FSD) and derivative to study proteins. In addition some tools such as fluoru-spectrophotometer were widely in biophysics and material science after a pioneering research of Kasha, Vavilov, Perrin, Weber, Stockes and Forster in 1951 (Lakowicz 2006).

2.2 Electromagnetic (EM) radiation.

Spectroscopy is the study of matter properties through interaction with different components of the electromagnetic spectrum (Banwell, C. N 1972). Electromagnetic radiation is composed of periodical oscillating electric field coupled with a perpendicular magnetic field oscillating at the same frequency. The wave moves in a direction normal to both fields.

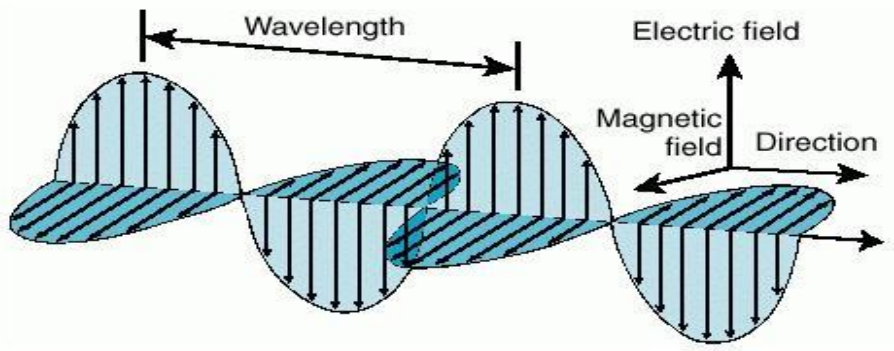

Figure 2.1: Electromagnetic wave representation (askthephysicist.com).

The EM spectrum can be divided into several frequency intervals. Each interval can be utilized by different spectroscopic techniques. EM spectrum extends from gamma (high energy waves), x-ray, and light down to radio frequencies (low energy waves) the infrared ranges is shown in figure 2.2.

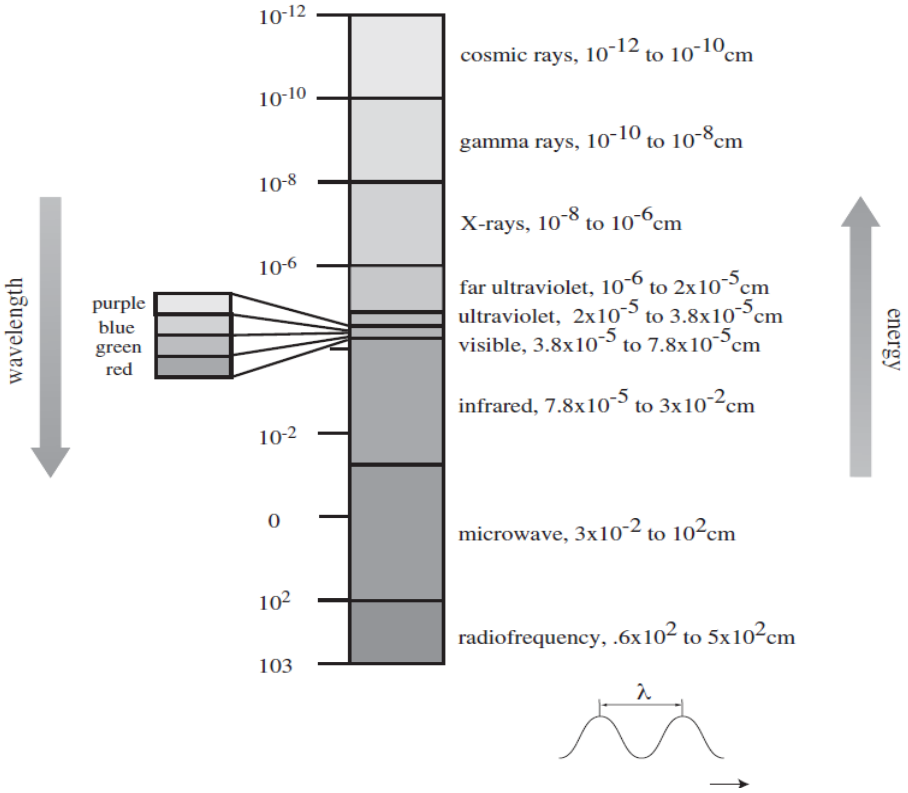

Figure 2.2: Electromagnetic spectrum (Shernan, M. 2014).

The IR wavelength range is 780 – $3x10^{5}$nm or .78-300 μm as shown in figure 2.3. The range is divided into near, mid and far IR. The UV wavelength range is .2-.38 μm. Our work utilizes the mid-IR from 3-30 μm where vibrational and rotational bands are observed, and the UV-VIS region from .01-.7 μm (Hollas J. M. 2004; Shernan, M. 2014).

In general, the spectrum gives information about the energy levels of the molecule, by observing which wavelengths a molecule absorbs, and to what extent it absorbs them. We can gain information about the nature of the energetic transitions that a molecule is able to undergo, and thus information about its structure.

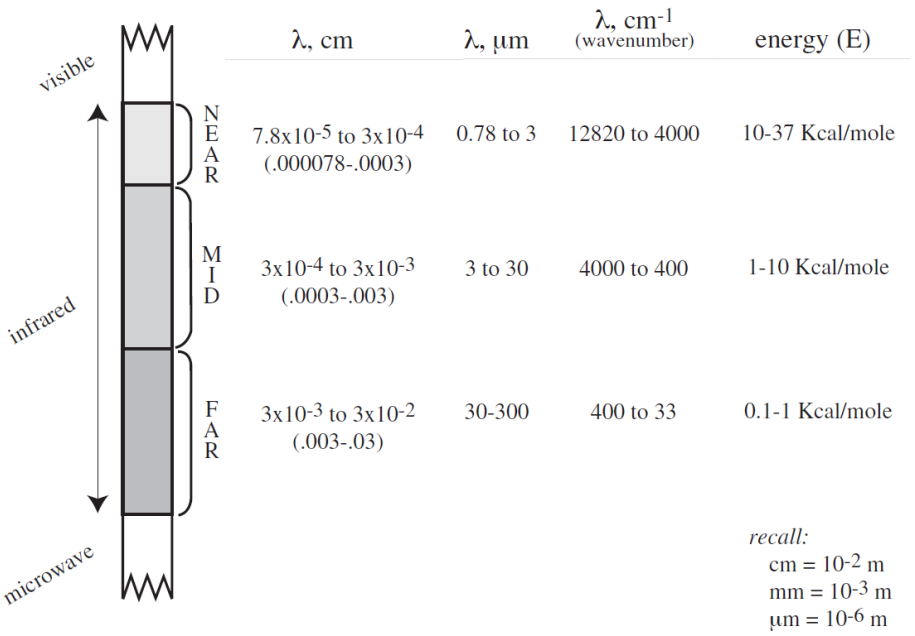

Figure 2.3: The IR region of electromagnetic spectrum (Shernan, M. 2014).

The spectrum consists of many lines because each level has a number of vibrational sublevels and each sublevel has a rotational spectrum, with a number of closely spaced wavelengths absorbed. The lines are too close to resolve and the absorption spectrum appears as a band or a broad peak (Hornaback, J.M. 2006).

Electromagnetic radiation and absorption can only occur at discrete energy levels due to the energy levels quantization. The absorbed EM radiation of by a molecule can change its electronic state causing electron transitions; the inter-nuclear distance of two or more atoms, or the molecule rotation around the molecule center of mass (OPUS Bruker manual version 5.5, 2004 BRUKER OPTIK GmbH).

The total energy of a molecule can be the sum of electronic, vibrational, and rotational contributions as described in the equation below (Coleman, P. B. 1993).

$$E_{total} = E_{ele} + E_{vib} + E_{rot} \quad (1)$$

The wave-numbers (inverse of the wavelength) at which an organic molecule absorbs radiation give information about the functional groups present in the molecule. Certain groups of atoms absorb energy and therefore, give rise to bands at approximately the same frequencies. The spectrum can be analyzed with the help of tables that correlate frequencies with functional groups.

2.3 Molecular Vibrations

Infrared spectroscopy provides measurements of molecular vibrations due to the specific absorption of infrared radiation by chemical bonds (Narhi, L.O 2013). The energy at peak absorption corresponds to a frequency of vibration of a part of a sample molecule. As the starting point for introducing the concept of harmonic vibrations, it is instructive to consider molecules as an array of point masses that are connected with each other by mass-less spring representing the intra-molecular interactions between the atoms (Wilson et al. 1955).

The simplest case is given by two masses, m_A and m_B, corresponding to diatomic molecule A-B. Upon displacement of the spheres along the x-axis by Δx from equilibrium position, a restoring force F_x acts on the spheres, according to Hooke's law is given by

$$F_x = -f\Delta x \qquad (2)$$

The potential energy V is given by

$$V = \tfrac{1}{2} f \Delta x^2 \qquad (3)$$

and the kinetic energy T of the oscillating motion is given as:

$$T = \tfrac{1}{2} \mu(\Delta x`)^2 \qquad (4)$$

Where μ is the reduced mass defined by:

$$\mu = \frac{mA \,.\, mB}{mA + mB} \qquad (5)$$

The total energy invariance implies that the sum of the first derivatives of V and T is equal to zero. This leads eventually to the Newton equation of motion

$$\frac{d^2 \Delta x}{dt} + \frac{f}{\mu} \Delta x = 0 \qquad (6)$$

The equation describes a harmonic motion with frequency is given by:

$$\omega = \sqrt{\frac{f}{\mu}} \qquad (7)$$

The circular frequency of the harmonic vibration increases when the strength of the bond increases and decreases with increasing masses of the atoms. We may express the circular frequency in wave-numbers (cm^{-1}) through dividing by 2πc

$$V = \frac{1}{2\pi c}\sqrt{\frac{f}{\mu}} \qquad (8)$$

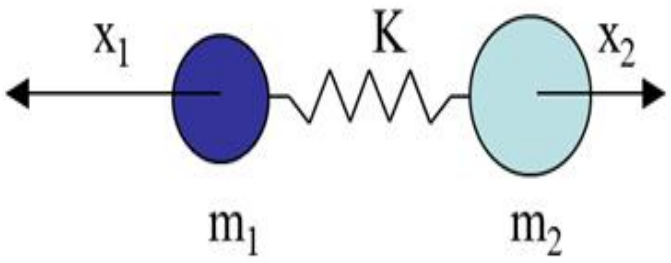

Figure 2.4: Diatomic molecule as a mass on a spring (bwtek.com).

2.3.1 Normal modes of vibrations

The normal modes are vibrational motions of the system, such that each coordinate of the system oscillates under simple harmonic motion with the same frequency (Rosman, B 2008). In the Cartesian coordinate system, each atom can be displaced in the x-, y- and z-directions, corresponding to three degrees of freedom.

A molecule of N atoms has a total of 3N degrees of freedom. Not all of them however correspond to vibrational degrees. A nonlinear molecule (the atoms are not located in straight line) has three rotational degrees, whereas there are only two for a linear molecule. The remaining 3N-6 and 3N-5 degrees correspond to the vibrations of a nonlinear and a linear molecule, respectively (Hildebrandt, P et al. 2008).

Degree of freedom type	Linear	Non-linear
Translational	3	3
Rotational	2	3
Vibrational	3N-5	3N-6
Total	3N	3N

Table 2.1: Degrees of freedom for polyatomic molecules (Stuart, B. 1997).

Stretching and bending are two types of molecular vibrations that correspond to the normal mode of a molecule. Stretching is a rhythmical movement along the bond axis and can be symmetric or anti-symmetric. Bending vibrations arise from a change in the bond angle between atoms or the movement of a group of atoms, relative to the remainder of the molecule (Mirabeela 1998). The frequency of normal modes is a characteristic of the presence of certain functional group. By examination of this frequency one can determine the functional groups present or absent (Shernan, M 2014).

Many of the group frequencies vary over a wide range because the bands arise from complex interacting vibrations within the molecule. Absorption bands may, however, represent predominantly a single vibrational mode. Certain absorption bands, for example, those arising from C-H, O-H, and C=O stretching modes, remain within fairly narrow regions of the spectrum.

2.3.2 Quantum mechanical treatment of vibrations

I. **The harmonic oscillator approximation** treats a diatomic as if the nuclei were held together by a spring. The quantum mechanical solution to the harmonic oscillator equation of motion set the energy spectrum values

$$E_v = (n+1/2)(h/2\pi)w \quad (9)$$

With $w = (f/\mu)^{1/2}$. The potential energy for diatomic molecule for harmonic oscillator approximation is shown in figure 2.5 (Banwell, C. N 1972).

II. The an-harmonic oscillator

Real molecules do not obey exactly the simple harmonic motion, real bonds do not follow hooks law they are not so elastic. If for example a bond stretches 60% of its real length then a molecular complicated situation should be assumed.

The Morse curve, for a molecule undergoing on harmonic extensional compression a purely empirical expression which fits this curve to good approximation was derived by P. Morse and is called the Morse function:

$$E= D_{eq} [1-\exp(a(r_{eq}-r))]^2 \quad (10)$$

With a = constant for a particular molecule, and D_{eq}= the dissociation energy. Using Schrodinger equation with $E=\frac{1}{2} f (r - r_{eq})^2$ the pattern of allowed vibration energy levels are

$$E_v= (v+\tfrac{1}{2})\hat{w}_e - (v+\tfrac{1}{2})^2 w_e x_e \quad cm^{-1}\ v =0,1,2 \quad (11)$$

Where w_e is the oscillating frequency and $\hat{w}_e$ is the oscillation frequency in wave number. x_e is the corresponding an-harmonicity constant which is positive and small for bond stretching in the order of 0.01. This means that the vibration levels will be crowded closely with increasing v (Banwell, C. N 1972).

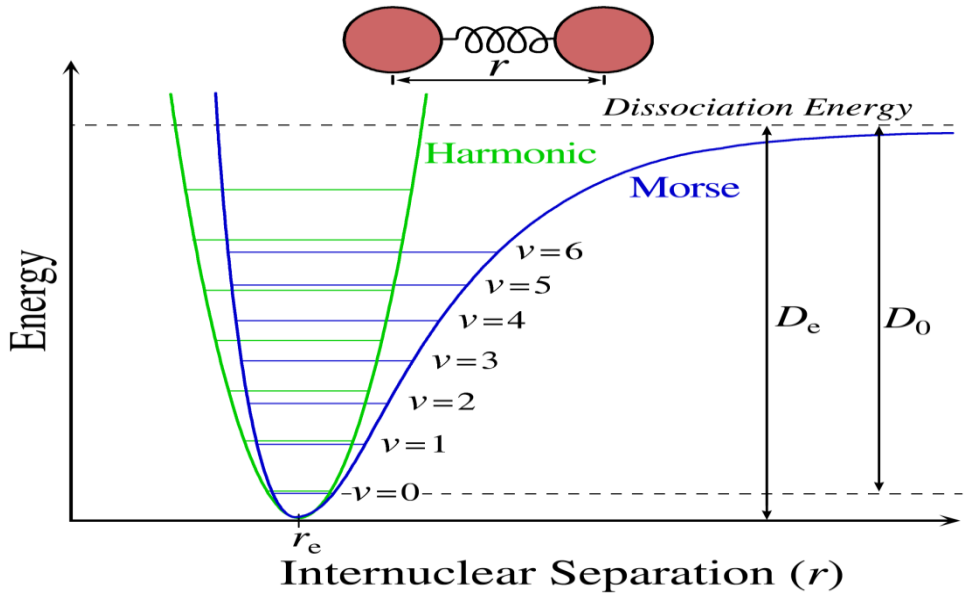

Figure 2.5: Potential energy of a diatomic molecule as a function of atomic displacement (inter-nuclear separation) during vibration. The Morse potential (blue) and harmonic oscillator potential (green) (Wikipedia: Vibronic spectroscopy).

2.4 FT-IR Spectroscopy

FT-IR spectroscopy is a measurement of wavelength and intensity of the absorption of IR radiation by a sample (Settle, F.A 1997). The old ways of spectroscopy were heavily dependent on dispersion elements such as prisms or gratings which limit the range of wave's length or energy selections. On the other hand Fourier Transform Spectroscopy allows simultaneous measurements at all frequencies and can be applied to both emission and absorption (Banwell, C. N 1972).

FT-IR spectroscopy has greatly extended the capabilities of infrared spectroscopy and was applied to many situations that are nearly impossible to analyze by dispersive instruments (Shernan. M 2014). The most important advantage of FT-IR spectroscopy for biological studies is that spectra of almost any biological system can be obtained in a wide variety of environments (Li et al 2007).

2.4.1 Infrared (IR) Spectroscopy

IR spectroscopy is one of the oldest and well established experimental and analytical techniques available to today's scientists (Settle, F. A, 1997). Simply, its absorption is measured at different IR frequencies by a sample positioned in the path of an IR beam. The main goal of IR spectroscopic analysis is to determine the chemical functional groups in the sample.

Different functional groups absorb characteristic frequencies of IR radiation. Using various sampling accessories, IR spectrometers can accept a wide range of sample types such as gases, liquids and solids. Thus, IR spectroscopy is an important and popular tool for structural elucidation and compound identification (Shernan. M 2014).

2.4.1.1 IR-Region

Infrared radiation is bound by the red end of the visible region at high frequencies and the microwave region at low frequencies (Shernan. M 2014). IR spectroscopists usually use the wave number which is directly proportional to frequency or the energy of the IR absorption. (Uversky, V. N et al. 2007; Shernan. M 2014).

The IR region is commonly divided into three smaller areas: near IR, mid IR and far IR. Mid-IR between 4000 and 400 cm^{-1} is the most frequently used region and it is what we have used in this study. The rough limits for each IR region are shown in the figure 2.6.

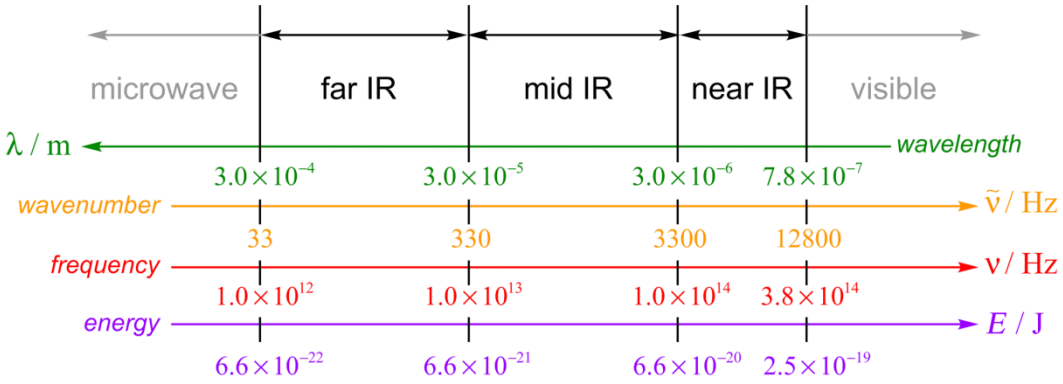

Figure 2.6: Regions of IR spectrum (benjamin-mills.com).

2.4.1.2 IR spectrum presentation

IR absorption information is generally presented in the form of a spectrum with wavelength or wave-number as the x-axis and absorption intensity or percent transmittance as the y-axis. Transmittance T, is the ratio of radiant power transmitted by the sample (I) to the radiant power incident on the sample (I_0). Absorbance (A) is the logarithm to the base 10 of the reciprocal of the transmittance (T).

$$A = \log_{10}(1/T) = -\log_{10} T = -\log_{10}(I/I_0) \qquad (12)$$

The transmittance spectra provide better contrast between intensities of strong and weak bands because transmittance ranges from 0 to 100% T whereas absorbance ranges from infinity to zero (Shernan. M 2014).

2.4.1.3 Principle of IR absorption

Absorption is the process by which the energy of a photon is taken up by the matter. There are several types of physical processes that could lie behind absorption, depending on the quantum energy of the particular frequency of EM radiation for example; ionization and electronic transitions. In case of energy absorption, molecules are excited to a higher energy states including IR absorption.

IR radiation does not have enough energy to induce electronic transitions as seen with UV and visible light. It corresponds to energy changes on the order of 8 to 40 KJ/mole. Absorption of IR is restricted to excite vibrational and rotational states of a molecule.

If the frequency of the radiation matches the vibrational frequency of the molecule then the radiation will be absorbed, causing a change in the amplitude of molecular vibration. However not all bonds in a molecule are capable of absorption infrared energy. Only if the vibrations or rotations within a molecule cause a net change in the dipole moment of the molecule the bond is capable to absorb IR (Pavia, D. L et al. 2009).

Infrared spectrum represents a fingerprint of a sample with absorption peaks which corresponds to the frequencies of vibrations between bonds of the atoms making up the material. Accordingly no two compounds produce the same infrared spectrum. Therefore, infrared spectroscopy can result in a positive identification (qualitative analysis) of various materials. In addition, the size of the peaks in the spectrum is a direct indication of the amount of material present (quantitative analysis) (Thermo Nicolet, 2001).

The height of the peaks is defined by the Beer-Lambert relationship. The concentration C is directly proportional to the absorbance A. That is:

$$A = abC \qquad (13)$$

Where (a) is the absorptivity of the molecule and b is the path length or distance that the light travels through the sample (Workman, 1998).

2.4.2 Theory of FT-IR spectroscopy

FT-IR is the preferred method of infrared spectroscopy. The resulting spectrum after IR passes through the sample represents the molecular absorption and transmission creating a molecular fingerprint of the sample (Thermo Nicolet, 2001). FT-IR spectrometer basically depends on a simple optical device called an interferometer. As shown in the figure below, the interferometer requires two mirrors, an infrared light source, an infrared detector and a beam splitter.

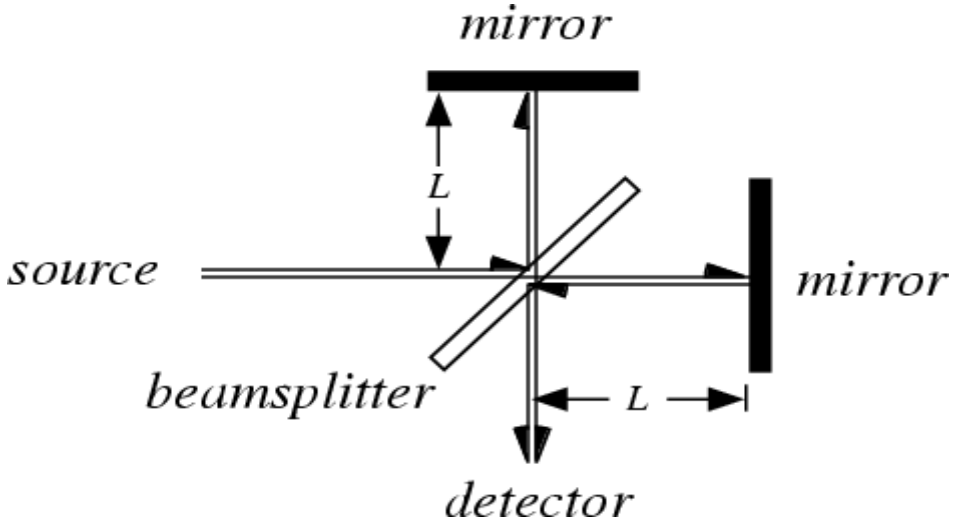

Figure 2.7: The Michelson interferometer (scienceworld.wolfram.com).

The beam-splitter is the heart of the interferometer. It is essentially a half-silvered mirror, and reflects about half of an incident light beam while simultaneously transmitting the remaining half. One half of this split light beam travels to the interferometer's moving mirror while the other half travels to the interferometer's stationary mirror. The two mirrors reflect both beams back to the beam-splitter where each of the two beams is again half reflected and half transmitted.

Two output beams result: one travels to the detector as the other travels to the source. When the two beams return to the beam-splitter, an interference pattern, or interfero-gram, is generated. This interference pattern varies with displacement of the moving mirror, or the difference in path length between the two arms of the interferometer. The interference pattern, detected by the infrared detector as variations in the infrared energy level, is what ultimately yields the spectral information (Hsieh, H. N 2008).

The interferogram is Fourier transformed to convert the space domain into a wave number domain (Viji 2006). The integral equation used in FT-IR spectroscopy can be obtained from the definition of Fourier integral theorem. For example the equation for the case of Michelson interferometer can be derived as follows: The amplitude of the wave (traveling in the z-direction) incident on the beam splitter is

$$E(z,v)\, dv = E_0(v)\, e^{i(\omega t - 2\pi vz)}\, dv \qquad (14)$$

Where $E_0(v)$ is the maximum amplitude of the beam at z=0. The amplitude of the beam is divided at the beam splitter and two beams are produced. Let $z_1$and z_2 be the distances traveled by the beams when they recombine. Each beam undergoes one reflection from the beam splitter and one transmission through the beam splitter. If *r* and *t* are the reflection and transmission coefficients, respectively, of the beam splitter, then the amplitude of the recombined wave E_R is

$$E_R\,[z_1,z_2,v]\, dv = rt\, E_0\,(v)\, [\, e^{i(\omega t - 2\pi v z_1)} + e^{i(\omega t - 2\pi v z_2)}]\, dv \qquad (15)$$

By definition, the intensity after recombination of the beams for the fixed spectral range dv is given by

$$I(z_1, z_2, v)\, dv = E_R\,(z_1, z_2, v)\, E_R^{*}(z_1, z_2, v)\, dv$$

$$= 2\, E_0^{2}\,(v)\, |rt|^2\, [1+ \cos 2(z_1-z_2)\, v]\, dv \qquad (16)$$

The total intensity at any path difference $x=(z_1-z_2)$ for the whole spectral range is obtained by integrating equation (16) as

$$I_R\,(x) = 2\,|rt|^2 \int_0^{\infty} E_0^{2}(v)\, dv + 2\,|rt|^2 \int_0^{\infty} E_0^{2}(v) \cos(2\pi xv) dv \qquad (17)$$

Fourier cosine transform of equation (17) converts intensity into spectrum as

$$E_0^{2}(v) = (\, 1/\, \pi|rt|^2) \int_0^{\infty} [I_R\,(x) - \tfrac{1}{2}\, I_R\,(0)] \cos(2\pi vx)\, dx \qquad (18)$$

$I_R\,(0)$ represents the flux associated with waves at zero arm displacement where the waves for all frequencies interact coherently. Thus, IR (0) is the flux associated with coherent interference and $I_R(x)$ is the flux associated at path difference x. [$I_R\,(x) - 1/2\, I_R(0)$] is called the interferogram. The spectrum *S(v),* which is proportional to $E_0^{2}(v)$ can be given from equation (18) as

$$S(v)\ \alpha\ E_0(v) = \text{constant} \int_0^{\infty} [I_R\,(x) - 1/2\, I_R\,(0)] \cos(2\pi vx)\, dx \qquad (19)$$

The interferogram is Fourier transformed with the help of computer to convert the space domain into the wave number domain (Cooper, A 2004).

2.4.3 Sample analysis by the FT-IR spectrometer.

1. **The Source:** Infrared energy is emitted from a glowing black-body source. This beam passes through an aperture which controls the amount of energy delivered to the sample (and, ultimately, to the detector).
2. **The Interferometer:** The beam enters the interferometer where the "spectral encoding" takes place. The resulting interferogram signal then exits the interferometer.
3. **The Sample:** The beam enters the sample compartment where it is transmitted through or reflected off of the surface of the sample, depending on the type of analysis being accomplished. This is where specific frequencies of energy, which are uniquely characteristic of the sample, are absorbed.
4. **The Detector:** The beam finally passes to the detector for final measurement. The detectors used are specially designed to measure the special interferogram signal.
5. **The Computer:** The measured signal is digitized and sent to the computer where the Fourier transformation takes place. The final infrared spectrum is then presented to the user for interpretation and any further manipulation (Thermo Nicolet 2001).

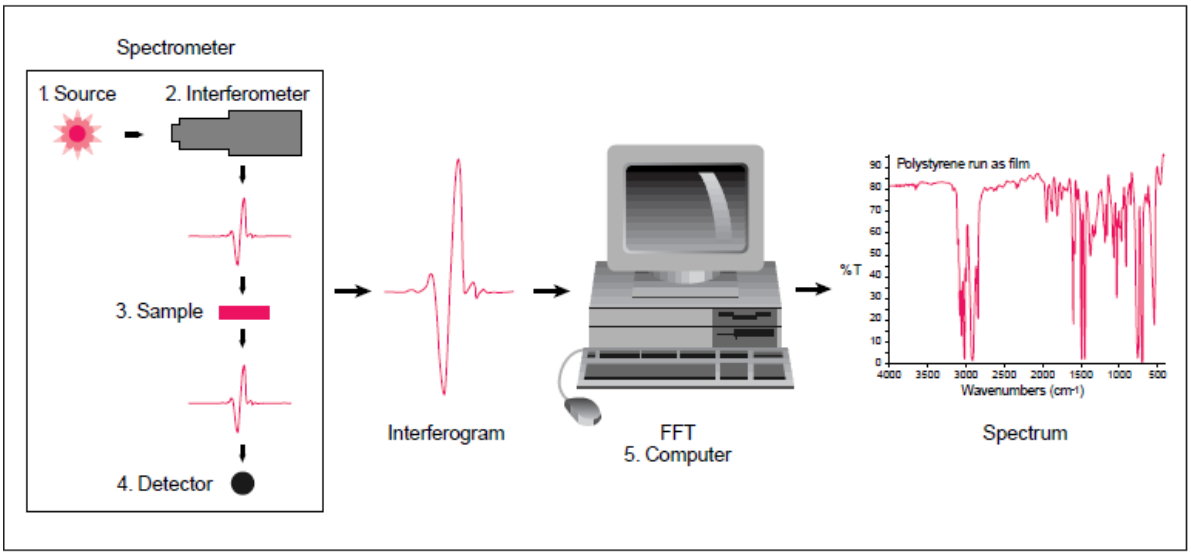

Figure 2.8: FT-IR spectrometer layout and basic components (chemwiki.ucdavis.edu).

2.5 Ultraviolet Visible (UV-VIS) Spectrophotometer

This absorption spectroscopy uses electromagnetic radiations between 190nm to 800 nm and is divided into the ultraviolet (UV 190-400 nm) and visible (VIS 400-800 nm) regions. Since the absorption of ultraviolet or visible radiation by a molecule leads transition among electronic energy levels of the molecule. It is also often called as electronic spectroscopy.

Nature of electronic transitions

Energy absorbed in the UV regions produces changes in the electronic energy of the molecule. As a molecule absorbs energy, an electron is promoted from an occupied molecular orbital (usually a non-bonding or bonding π orbital) to an unoccupied molecular orbital) an anti-bonding π* or σ* orbital) of greater potential energy, as in figure 2.8.

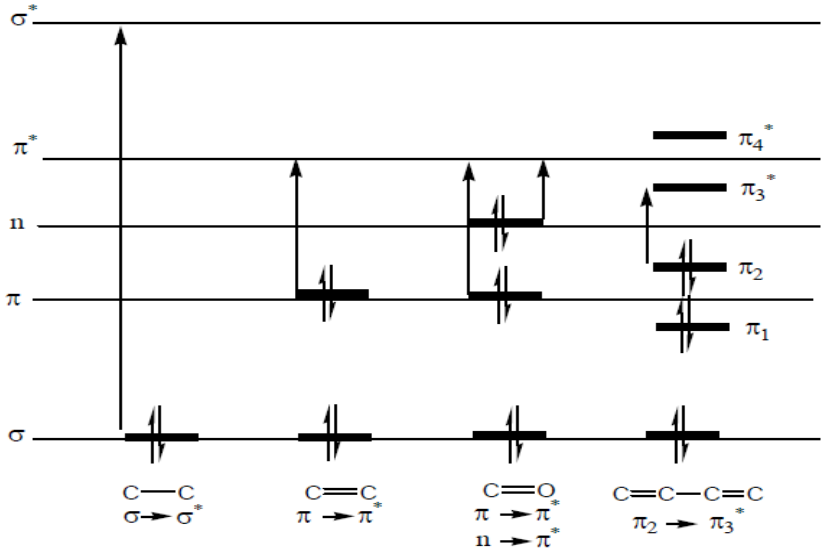

Figure 2.8: Relative energies of orbitals most commonly involved in electronic spectroscopy of organic molecules (Prof. Subodh Kumar. 2006).

For most molecules, the lowest energy occupied molecular orbitals are σ orbitals, which correspond to σ bonds. So the possible electronic transitions are:

$$n \rightarrow \pi^* < n \rightarrow \sigma^* < \pi \rightarrow \pi^* < \sigma \rightarrow \pi^* < \sigma \rightarrow \sigma^*$$

The energy of radiation being absorbed during excitation of electrons from ground state to excited state primarily depends on the nuclei that hold the electrons together in a bond. The group of atoms containing electrons responsible for the absorption is called chromophore (Hildebrandt, P & Siebert, F 2008).

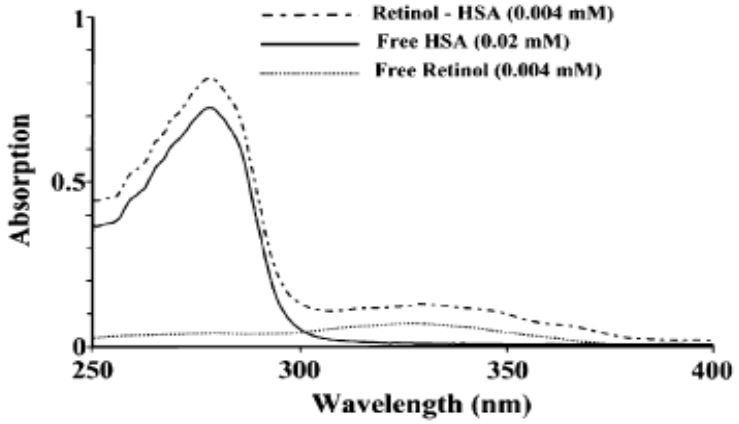

Figure 2.10: UV-absorption spectra of free HSA (0.02 mM), free retinol (0.004 mM) and their protein complexes (Prof. Subodh Kumar. 2006).

By assuming that there is only one type of interaction between testosterone and HSA in aqueous solution, leads to establish Equations. (20) and (21) as follows:

HSA + Testosterone $\longleftrightarrow$ Testosterone: HSA (20)

K = [Testosterone: HSA]/ [Testosterone][HSA] (21)

The absorption data were handled using linear double reciprocal plots based on the following equation (Rosman, B 2008):

$$\frac{1}{A-A_0} = \frac{1}{A_\infty - A_0} + \frac{1}{K[A_\infty - A_0]} \cdot \frac{1}{L} \quad (22)$$

A_0 corresponds to the initial absorption of protein at 280 nm in the absence of ligand, A_∞ is the final absorption of the ligated protein, and A is the recorded absorption at different Testosterone concentrations (L).

The double reciprocal plot of 1/ (A - A_0) vs. 1/L is linear and the binding constant (K) can be estimated from the ratio of the intercept to the slope. From the value obtained we can determine if the binding between HSA and Testosterone is weak or strong by comparing it to the complex constants for strongly bound ligand–protein complexes vary within the range 10^6 to 10^8 M^{-1} (Hornaback, J.M 2006).

A spectrometer is an instrument that measures the intensity of a light beam as a function of wavelength. Spectrophotometers for the measurement of absorbance in the UV/VIS range come in a variety of configurations. The most common routine laboratory instruments are

single- or double beam devices made up of a light source, monochromatic, sample compartment, detector, data processor and display (Cooper 2004).

The absorption of UV waves by proteins has been analyzed in detail and proposed as a structural probe from the early days of molecular biology. The absorption of proteins in the UV arises mainly from electronic bands in aromatic amino acid side chains (tryptophan, tyrosine, phenylalanine) and ,to a lesser extent, cysteine residues, close to 280 n (Serduyk et al. 2007).

2.6 Fluorescence Spectrophotometer

Fluorescence Spectrophotometry is a class of techniques that examines the state of biological systems by studying its interactions with fluorescent probe molecules (Dong, C. Y & So, P. T 2002). Luminescence is the emission of light by a substance not resulting from heat. It is a form of cold body radiation. Luminescence is formally divided into two categories fluorescence and phosphorescence depending on the nature of the excited states (Soukpo´e-Kossi et al 2007).

Fluorescence and phosphorescence occur during molecular relaxation from electronic excited states. Fluorescence is the emission of light by a substance that has absorbed light or other electromagnetic radiation (Johnson. L & Spence. T. Z. M 2010).

Fluorophores are molecules capable of fluorescing. In its ground state, the fluorophore molecule is in a relatively low energy, stable configuration, and it does not fluoresce. Fluorophores are unstable at high energy configurations, and they decay eventually to the semi-stable lowest-energy excited state. The process responsible for the fluorescence is illustrated by the Jablonski diagram shown in Figure 2.10, where E denotes the energy scale, S_0 is the ground singlet electronic state, S_1 and S_2 are the successively higher energy excited singlet electronic states and T_1 is the lowest energy triplet state (Dong, C.Y & So, P.T 2002).

The fluorescence lifetime and quantum yield are the most important characteristics of a fluorophore. Quantum yield is the number of emitted photons relative to the number of absorbed photons. The fluorophore lifetime is determined by the time available for

interaction or diffusion with environment, and hence the information available from its emission (Lakowicz 2006).

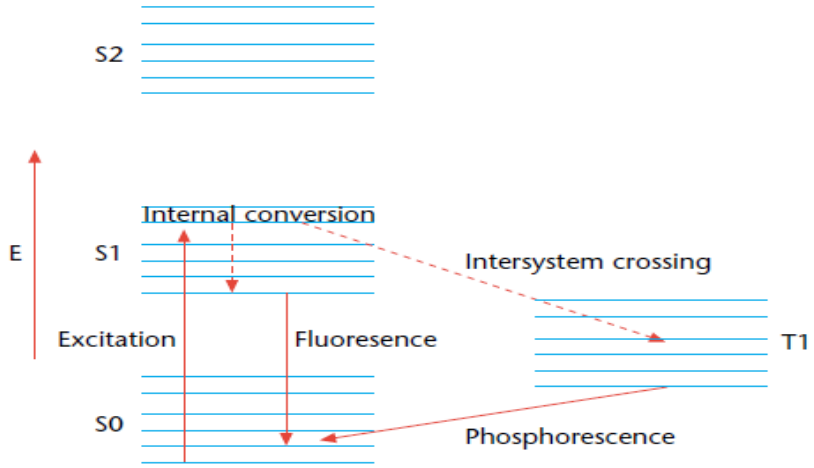

Figure 2.10: The Jablonski diagram of fluorophore excitation (Dong, C.Y & So, P.T 2002).

Fluorophores are divided into two main classes. One is the intrinsic fluorophores that occur naturally, such as aromatic amino acids. The other is extrinsic fluorophore that is added to the sample to provide fluorescence when none exists, or change the spectral properties of the sample (Lakowicz 2006). After the excitation occurs, the state exists for a finite time (typically 1-10 nanoseconds).

During this stage the fluorophore undergoes conformational changes and it is also subject to a multitude of possible interactions with its molecular environment. These processes have two important consequences. 1) The energy of S_2 is partially dissipated, yielding a relaxed singlet excited state (S_1) from which fluorescence emission originates. 2) Not all the molecules initially excited by absorption return to the ground state (S_0) by fluorescence emission.

At **Fluorescence Emission stage,** a photon of energy $h\upsilon_{em}$ is emitted, returning the fluorophore to its ground state S_0. Due to energy dissipation during the excited-state lifetime, the energy of this photon is lower, and therefore of longer wavelength, than the excitation photon $h\upsilon_{ex}$. The difference in energy ($h\upsilon_{ex} - h\upsilon_{em}$) is called the Stokes shift (Johnson. L & Spence. T. Z. M 2010).

Fluorescence Quenching

Fluorescence quenching is a bimolecular process that reduces the fluorescence intensity without changing the fluorescence emission spectrum. It can result from transient excited-state interactions (collision quenching) or the formation of non-fluorescent ground-state species. For collision quenching the decrease in intensity is described by the well-known Stern-Volmer equation:

$$\frac{F_0}{F} = 1 + k_q \tau_0 [Q] \qquad (23)$$

K which will be calculated in the results represents the Stern-Volmer quenching constant, k_q is the bimolecular quenching constant, τ is the unquenched lifetime, and [Q] is the quencher concentration. F is the fluorescence intensity after adding the quencher which is here testosterone and F0 is the fluorescence intensity before quenching.

The Stern-Volmer quenching constant K indicates the sensitivity of the fluorophore to a quencher. A fluorophore buried in a macromolecule is usually inaccessible to water soluble quenchers, so that the value of K is low. Larger values of K are found if the fluorophore is free in solution or on the surface of a biomolecule.

Fluorescence spectroscopy can be applied to a wide range of problems in the chemical and biological sciences. The measurements can provide information on a wide range of molecular processes, including the interactions of solvent molecules with fluorophores, conformational changes, and binding interactions (Lakowicz, J. R 2006).

The fluorescence of HSA results from the tryptophan, tyrosine, and phenylalanine residues. The intrinsic fluorescence of many proteins is mainly contributed by tryptophan alone, because phenylalanine has very low quantum yield and the fluorescence of tyrosine is almost totally quenched if it is ionized or near an amino group, a carboxyl group, or a tryptophan residue (Darwish et al. 2010).

The maximum value for the dynamic bimolecular quenching constant is ($2.0\times10^{10}\ M^{-1}\ s^{-1}$) (Litwack. G & Axelord. J 1970) and the fluorescence life time is about 10^{-8}s. If the quenching constant is larger than the maximum value the quenching is static and we can use the equation:

$$\frac{1}{F_0 - F} = \frac{1}{F_0 K(L)} + \frac{1}{F_0} \qquad (24)$$

K is the binding constant of testosterone with HSA. When we plot 1/ (F_0– F) Vs. 1/ L we can get the value of the binding constant from the slope and the intercept (Brandt 1999).

2.7 Proteins

Proteins are important organic chemical substances in our life and represent a major target for many types of medications in our body (Zhang, G et al. 2008).

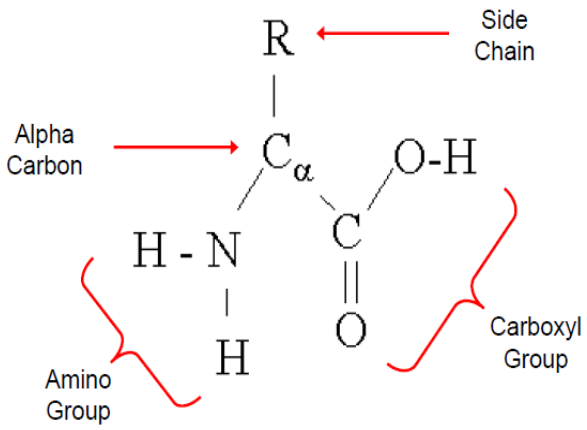

Figure 2.11: Amino acid structure (Nelson DL, Cox MM 2005).

Proteins are found in every single living. They are polymers consisting of amino acids linked by peptide bonds. They perform a vast array of functions including catalyzing metabolic reactions, replicating DNA, responding to organisms, and transporting molecules (Nelson DL, Cox MM 2005).

Each amino acid consists of a central carbon atom (alpha-carbon), an amino group (NH2), a carboxyl group (COOH) and a side chain. The differences in side chains distinguish different amino acids (Colin, D 2014).

2.7.1 Protein Structure

Protein chemical structure and molecular conformation are commonly described in terms of four levels: primary, secondary, tertiary and quaternary structures.

The primary structure refers to a linear sequence of amino acids. It is sometimes called the "covalent structure" of proteins because most of the covalent bonding within proteins defines the primary structure (Gorga, F. R 2007).

The secondary structure is the result of hydrogen bonds between the repeating constituents of the polypeptide backbone (not the amino acid side chains). Within the backbone, the oxygen atoms have a partial negative charge, and the hydrogen atoms attached to the nitrogen have a partial positive charge. Therefore, hydrogen bonds can form between these atoms. Individually, these hydrogen bonds are weak, but because they are repeated many times over a relatively long region of the polypeptide chain, they can support a particular shape for that part of the protein (Reece, J. B et al 2011).

The two most common secondary structure elements are the following

The Alpha Helix is the most common structural motif found in proteins. In globular proteins over 30 percent of all residues are found in helices (Whitford, D 2005). It is a cylindrical shape formed by a coiling of the polypeptide chain on itself with interactions take place between groups 3-4 amino acid residues apart. (Hydrogen bonds between the hydrogen atoms attached to the amide nitrogen and the carbonyl oxygen atom). The first four NH groups and last four CO groups will normally lack backbone hydrogen bonds (Gropper, S. S et al. 2009).

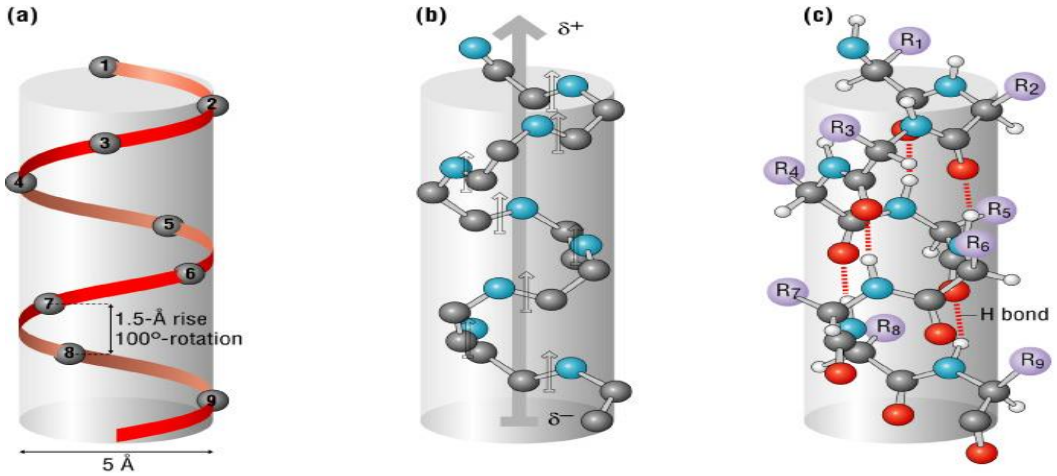

Figure 2.12: Alpha Helix Protein (Gropper, S. S et al. 2009).

In the Beta Pleated Sheet structure, the polypeptide chain is fully stretched out with the side chains positioned either up or down. The stretched polypeptide can fold back on itself with its segments packed together (Gropper, S. S et al 2009).

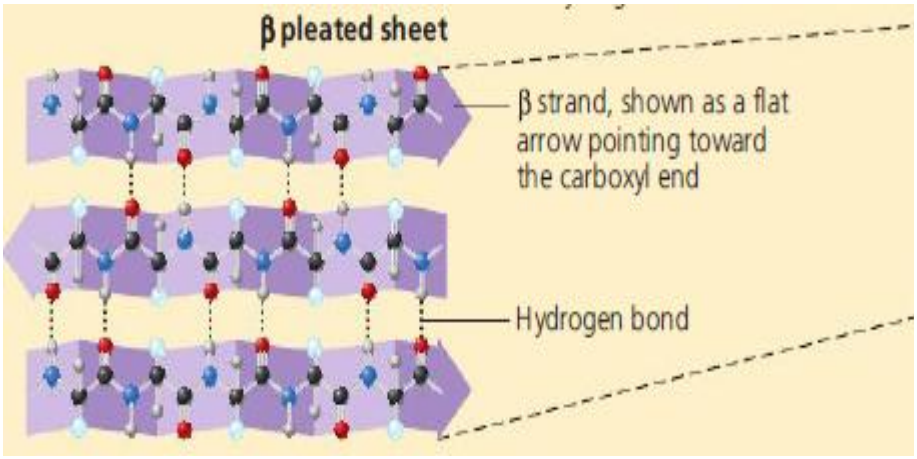

Figure 2.13: Beta Pleated Sheet (Gropper, S. S et al 2009).

β strands can interact in either parallel or anti-parallel orientations, and each form has a distinctive pattern of hydrogen bonding. Figures (2.14 and 2.15) illustrate examples of anti-parallel and parallel β sheets from real protein structures.

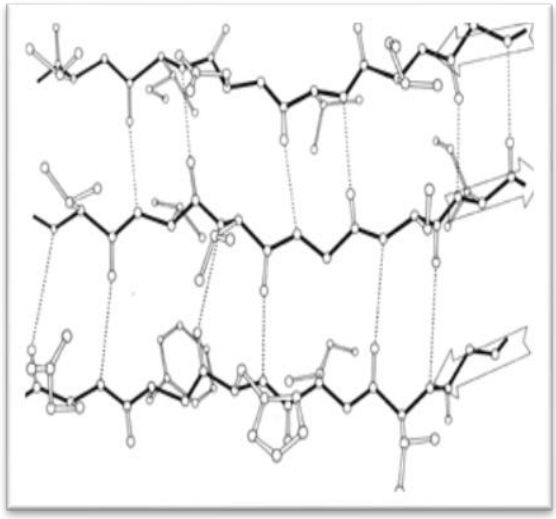

Figure 2.14: Anti parallel Beta Pleated Sheet Protein (Richardson, J.S 2007).

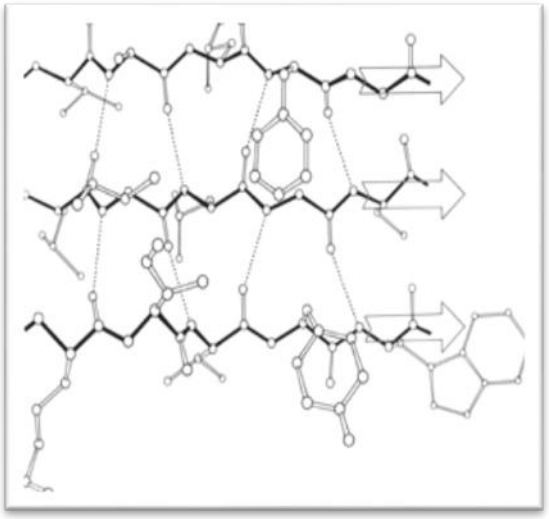

Figure 2.15: Parallel Beta Pleated Sheet Protein (Richardson, J.S 2007).

The anti-parallel sheet has hydrogen bonds perpendicular to the strands, and narrowly spaced bond pairs alternate with widely spaced pairs. Looking from the N- to C-terminal direction along the strand, when the side chain points up the narrow pair of H bonds will point to the right. Parallel sheet has evenly spaced hydrogen bonds (Richardson, J.S 2007). There are other secondary structure elements such as turns, coils, 3_{10} helices, etc.

The Tertiary Structure describes the way in which the elements of protein secondary structures are arranged in space

The Quaternary Structure describes how several polypeptide chains come together to form a single functional protein (Cooper, 2004).

2.7.2 Human Serum Albumin (HSA)

Human Serum Albumin HSA is an abundant plasma protein that binds a wide variety of hydrophobic ligands including fatty acids, bilirubin, thyroxin and hemin and also drugs (Carter D. C. et al 1989). The most important physiological role for the protein is to bring such solutes into the blood stream and then deliver them to the target organs, as well as to maintain the pH and osmotic pressure of plasma (Abu Teir et al 2010; Abu Teir et al 2014). HSA concentration in the blood is 40 mg/ml.

The three dimensional structure of HSA was determined through x-ray crystallographic measurements (Carter D. C. et al, 1989). This globular protein is of Molecular weight 65 K and consists of 585 amino acids. Its amino-acid sequence contains a total of 17 disulphide bridges, one free thiol (Cys 34), and a single tryptophan (Trp 214). The disulphides are positioned in a repeating series of nine loop-link-loop structures centered on eight sequential Cys-Cys pairs (Min-He X, Carter D. C, 1992).

It became evident from early heavy-atom derivative screens and preliminary binding studies that the principal binding regions of HSA are located in sub-domains I, II and III each containing two sub domains (A&B) and stabilized by 17 disulphide bridges (Min-He, X & Carter D.C. 1992; Ouameur et al. 2004).

Aromatic and heterocyclic ligands were found to bind within two hydrophobic pockets in sub-domains IIA and IIIA, which are site I and site II. Site I is dominated by strong hydrophobic interaction with most neutral, bulky, heterocyclic compounds, while site II mainly dipole-dipole, Van der Waals, and/or hydrogen-bonding interactions with many aromatic carboxylic acids (Ouameur et al. 2004). HSA contained a single tryptophan residue (Trp 214) in domain IIA and its intrinsic fluorescence is sensitive to the ligands bounded nearby (Krishna Kumar 2002, II'ichrv 2002). It is often used as a probe to investigate the binding properties of drugs with HSA.

The distribution of free concentration and the metabolism of various drugs can be significantly altered as a result of their binding to HSA (Kang J et al. 2004).The binding

properties of albumin depend on the three dimensional structure of the binding sites which are distributed over the molecule. Strong binding can decrease the concentrations of free drugs in plasma, whereas weak binding can lead to a short lifetime or poor distribution.

Its remarkable capacity to bind a variety of drugs results in its prevailing role in drug pharmacokinetics and pharmacodynamics (Kandagal P. B et al 2007). Multiple drug binding sites for HSA were reported by several researchers (Bhattacharya, A et al. 2000).

The distribution and metabolism of many biologically active compounds whether drugs or natural products are correlated with their affinities toward serum albumin which is the most abundant protein carrier in the plasma. The study of the interaction of such molecules (for example: testosterone with albumin) has a valid importance.

Some investigations of the Testosterone-HSA interaction were conducted but none determined either Testosterone-HSA binding constant k or the effect of testosterone complexes on the protein structure, as we studied in this research. Some investigations only indicated that the interaction occurred and others used the equilibrium dialysis method to calculate the binding constant (Ouameur, A. A et al. 2004) (IUPAC 2012).

Testosterone does not dissolve in blood plasma, which is mainly water. It does need a hydrophilic carrier to move in the blood to reach the target tissues. On the other hand HSA is considered a universal carrier to hydrophobic molecules when it binds with testosterone, cholesterol and progesterone. In the case of abnormal testosterone concentration regardless of source, studying testosterone-HSA interaction and how it affects the protein structure may help in determining the possibilities the hormones disorders by comparing the normal and high concentration testosterone cases.

HSA affinity to bind with other molecules and drugs may be affected by increasing Testosterone-HSA binding. This may cause shortage of supplying the target tissues with certain molecules. Accordingly we need to understand this interaction to help identify the scope of the above question.

Chapter Three

Experimental Setup and Measurements

Chapter Three

Experimental Setup and Measurements

Section one contains information about samples and film preparation. Section two includes a description of the spectrometers used in this work, namely Bruker IFS 66/S FT-IR spectrophotometer, UV-VIS spectrophotometer (NanoDrop ND-1000) and Fluoro Spectrometer (NanoDrop 3300). Section three reviews the experimental procedure.

3.1 Samples and Materials

HSA (fatty acid free) testosterone in powder form were purchased from Sigma Aldrich chemical company and used without further purifications. The data were collected using samples in the form of thin films for FT-IR measurements and liquid form for UV-VIS and fluorescence measurements. Preparation of the thin film samples required several stock solutions as described below.

3.1.1 Preparation of HSA stock solution

HSA was dissolved in phosphate buffer saline at physiological pH 7.4 to a concentration of 80 mg/ml, to get a final concentration of 40 mg/ml in the final hormone-HSA solution.

3.1.2 Preparation of testosterone stock solution

Testosterone (molecular weight 288.42 g/mol) was dissolved in phosphate buffer saline (0.7622 mg/ml) at room temperature. The solution was placed on a shaker for one hour in order to dissolve the testosterone powder with buffer, then it was placed in ultrasonic water path (SIBATA AU-3T) for 8 hours to ensure that the entire amount of testosterone was completely dissolved. The solution was placed in a water path with a temperature range 37-40c° for one hour to completely dissolve it and make it homogenous.

3.1.3 HSA-Testosterone solutions

The final concentrations of HSA-Testosterone solutions were prepared by mixing equal volume of HSA and testosterone to form the HSA-Hormone complexes.The HSA concentration in all samples was kept at 40 mg/ml. However, the hormone concentration in the final solutions was reduced such that the molecular ratios (HSA: Testosterone) are 10:18, 10:14, 10:10, 10:6 and 10:2.

3.1.4 Thin film preparation

Silicon windows (NICODOM Ltd) were used as spectroscopic cell windows. The optical transmission is high with little or no distortion of the transmitted signal. The 100% line of NICODOM silicon window shows that the silicon bands in the mid-IR region do not exhibit total absorption and can be easily subtracted. 60 µl of each sample of HSA-Testosterone was spread on a silicon window and an incubator was used to evaporate the solvent, to obtain a transparent thin film on the silicon window. All solutions were prepared at the same time at room temperature.

3.2 Instruments

We used the following instruments for our experiment

3.2.1 FT-IR Spectrometer

The FT-IR measurements were obtained using a Bruker IFS 66/S spectrophotometer equipped with a liquid nitrogen-cooled MCT detector and a KBr beam splitter. The spectrometer was continuously purged with dry air during the measurements.

3.2.2 UV-VIS spectrophotometer (NanoDrop ND-1000)

The absorption spectra were obtained using a NanoDrop ND-1000 spectrophotometer to measure the absorption spectrum of the samples in the range between 220-750 nm, with high accuracy and reproducibility.

3.2.3 Fluorospectrometer (NanoDrop 3300)

The fluorescence measurements were performed by a NanoDrop ND-3300 Fluorospectrophotometer at 25°C. The excitation source was one of three solid-state light emitting diodes (LED's). The excitation source options include: UV LED with maximum excitation 365 nm, Blue LED with excitation 470 nm, and white LED from 500 to 650nm excitation. A 2048-element CCD array detector covering 400-750 nm, was connected by an optical fiber to the optical measurement surface. The excitation was made at the wavelength of 360nm and the maximum emission wavelength was 439nm. Other equipment such as Digital balance, pH meter, Vortex, Plate stir and Micropipettes were used (NanoDrop 3300 Fluorospectrometer V2.7 user's Manual 2008).

3.3 Experimental procedure

3.3.1 UV-VIS spectrophotometer experimental procedures.

The UV-VIS spectrophotometer procedure was followed as described in NanoDrop1000 User's Manual (NanoDrop 1000 Spectrophotometer V3.7, User's Manual, 2008) as follows

Operation

A 1µl sample of testosterone was pipetted into the end of a fiber optic cable (the receiving fiber). A second fiber optic cable (the source fiber) was then brought into contact with the liquid sample causing the liquid to bridge the gap between the fiber optic ends. The gap was controlled to both 1mm and 0.2 mm paths. A pulsed xenon flash lamp provided the light source and a spectrophotometer utilizing a linear CCD array was used to analyze the light after passing through the sample. The instrument was controlled by PC based software, and the data was logged in an active file on the PC.

Before taking the samples absorbance by the NanoDrop 1000 Spectrophotometer it was s calibrated or "blanked" by taking and storing the spectrum of a reference material (blank) in the memory of the instrument as an array of light intensities vs wavelength. When a measurement of a sample is taken, the intensity of light transmitted through the sample is recorded. The sample intensities along with the blank intensities were used to calculate the sample absorbance according to the following equation:

Absorbance = -log (Intensity sample/Intensity blank) (25)

The measured light intensity of for both the blank and the sample are required to calculate the absorbance at a given wavelength, and Beer-Lambert equation is used to correlate the calculated absorbance with concentration.

Basic Use: the main steps for using the sample retention system are listed below:

1. With the sampling arm open, pipette the sample onto the lower measurement pedestal. Photo 1 of Figure 3.1.
2. Close the sampling arm and initiate a spectral measurement using the operating software on the PC. The column is automatically drawn between the upper and lower measurement pedestals and the spectral measurement made. Photo 2 of Figure 3.1.
3. When the measurement is complete, open the sampling arm and wipe the sample from both the upper and lower pedestals using a soft laboratory wipe. Simple wiping

prevents carryover from successive measurements varying by more than 1000 fold in concentration. Photo 3 of Figure 3.1.

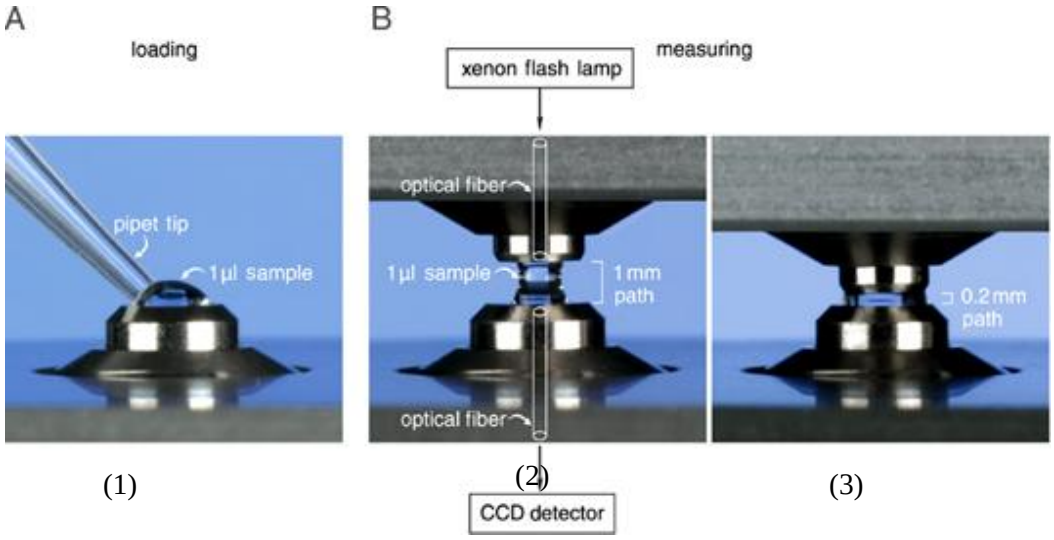

Figure 3.1: Main steps for using the sample UV-VIS Spectrophotometer (NanoDrop 1000).

3.3.2 Fluorospectrophotometer experimental procedures.

The Fluorospectrophotometer Procedure was followed as described in NanoDrop 3300 User's Manual (NanoDrop 3300 Fluorospectrometer V2.7 User's Manual, 2008) as follows: Before taking the measurements of samples the NanoDrop 3300 Fluorospectrometer was "blanked".

Operation

A 2.5 µl sample of testosterone was pipetted onto the end of the lower measurement pedestal (the receiving fiber). A non-reflective "bushing" attached to the arm is then brought into contact with the liquid sample causing the liquid to bridge the gap between it and the receiving fiber. The gap, or path-length controlled to 1mm. Following the excitation with one of the three LED the light from the sample passing through the receiving fiber was captured by the spectrophotometer. The NanoDrop 3300 was controlled, logged and archived by computer software.

Basic Use: The main steps for making measurements are listed below:

1. With the sampling arm open, pipette the sample into the lower measurement pedestal Photo 1 of Figure 3.2.

2. Close the sampling arm and initiate a measurement using the computer software. The sample column is automatically drawn between the upper bushing and the lower measurement pedestal and the measurement is made. Photo 2 of Figure 3.2.
3. When the measurement is complete, open the sampling arm and wipe the sample from both the upper bushing and the lower pedestal using low lint laboratory wipe. Photo 3 of Figure 3.2.

Figure 3.2: Main steps for using the sample Fluorospectrophotometer (NanoDrop 3300).

3.3.3 FT-IR Spectrometer experimental procedures

The absorption spectra were obtained for wave numbers in range of 400-4000 cm^{-1}. A spectrum was taken as an average of 60 scans to increase the signal to noise ratio, and the spectral resolution was at 4 cm^{-1}. The aperture used in this study was 8 mm. We found that this aperture gives the best signal to noise ratio. Baseline correction, normalization and peak areas calculations were performed for all the spectra by OPUS software. The peak positions were determined using the second derivative of the spectra.

The infrared spectra of HSA, Testosterone-HSA were obtained for wave numbers in the range 1000-1800 cm^{-1}. The FT-IR spectrum of free HSA was acquired by subtracting the absorption spectrum of the buffer solution from the spectrum of the protein solution. For the net interaction effect, the difference spectra {protein and testosterone solution - protein

solution} were generated using the featureless region of the protein solution 1800-2200 cm^{-1} as an internal standard (Surewicz et al. 1993).

3.3.4 FT-IR data processing

The analysis of IR spectra in terms of protein structure is not straightforward and present serious conceptual and practical problem, despite the well-recognized conformational sensitivity of the IR-active bonds. Bands in amide I, amide II and amide III regions are broad, not resolved into individual components corresponding to different secondary structure elements.

Resolution enhancement or band-narrowing methods are applied to resolve broad overlapped bands into individual bands. FT-IR spectroscopy presents several advantages over conventional dispersive techniques for this type of analysis through the application of second derivative, peak picking, spectral subtraction, baseline correction, smoothing, integration, curve fitting and Fourier self de convolution. In the present study several data processing tasks were used.

3.3.3.1 Baseline correction

The baseline correction method applied here includes two steps. The first step is to recognize the baseline. This was done by selecting a point from spectral points on the spectrum. Then adding or subtracting intensity value from the point or points to correct the baseline offset. Baseline correction task is used to bring the minimum point to zero. This was done automatically using Optic User Software (OPUS) and successfully removes most baseline offsets (Griffiths et al. 2007; OPUS Bruker manual, 2004).

3.3.3.2 Peak picking

Automated peak picking involves two steps: The recognition of peaks, and the determination of the wave-numbers of maximum or minimum absorbance. A threshold absorbance value is set so that weak bands are not measured (Griffiths et al., 2007).

3.3.3.3 Second derivative

Increased separation of the overlapping bands can be achieved by calculating the second derivative rate of change of slope of the absorption spectrum, second –derivative

procedure have been successfully applied in the qualitative study of a large number of proteins (Haris et al. 1999).

3.3.3.4 Fourier self-deconvolution

The Fourier deconvolution procedure, sometimes referred to as 'resolution enhancement' is the most widely used bands narrowing technique in infrared spectroscopy of biological materials (Jackson et al. 1981). Both second-derivative and deconvolution procedures have been successfully applied in the qualitative study of a large number of protein (Workman 1998; Kauppinnen et al. 1981). In addition to providing valuable information about their secondary structure, the method is useful for detecting conformational changes arising as a result of a ligand binding, pH, temperature, organic solvents, detergents, etc.

In many cases results obtained using this approach was supported by studies using other techniques such as X-ray diffraction and NMR. However, both derivative and deconvolution techniques should be applied with care since they amplify the noise significantly (Haris et al. 1999).

3.3.3.5 Spectral subtraction

Difference spectroscopy is another approach that is very useful for investigating subtle differences in protein structure. The principle of difference spectroscopy involves the subtraction of a protein absorbance spectrum in state A from that of the protein in state B. The resultant difference spectrum only shows peaks that are associated with groups involved in the conformational change (Goormaghtigh et al. 2006; Haris et al. 1999). The accuracy of this subtraction method was tested using several control samples with the same protein or drug concentrations and resulted into a flat base line formation.

3.3.3.6 Curve Fitting

The Curve Fit command allows calculating single components in a system of overlapping bands. A model consisting of an estimated number of bands and a baseline should be generated before the fitting calculation starts. The model can be set up interactively on the display and optimized during the calculation (OPUS Bruker manual, 2004).

Chapter Four

Results and Discussion

Chapter Four

Results and Discussion

In the first section, UV-VIS spectrophotometer results are discussed and analyzed. The next section deals with fluorescence spectrophotometer results. In the final section, FT-IR graphs and data analysis are given.

4.1 UV-VIS spectrophotometer

Many researchers have reported the effective use of UV-VIS spectroscopy to investigate the interaction of drugs with HSA (Dukor et al. 2001; Abu Teir et al. 2010; Azimi et al. 2011). The absorption spectra of different ratios of testosterone with fixed amount of HSA are displayed in Figure 4.1.The excitation was on 210nm and the absorption was recorded at 278 nm.

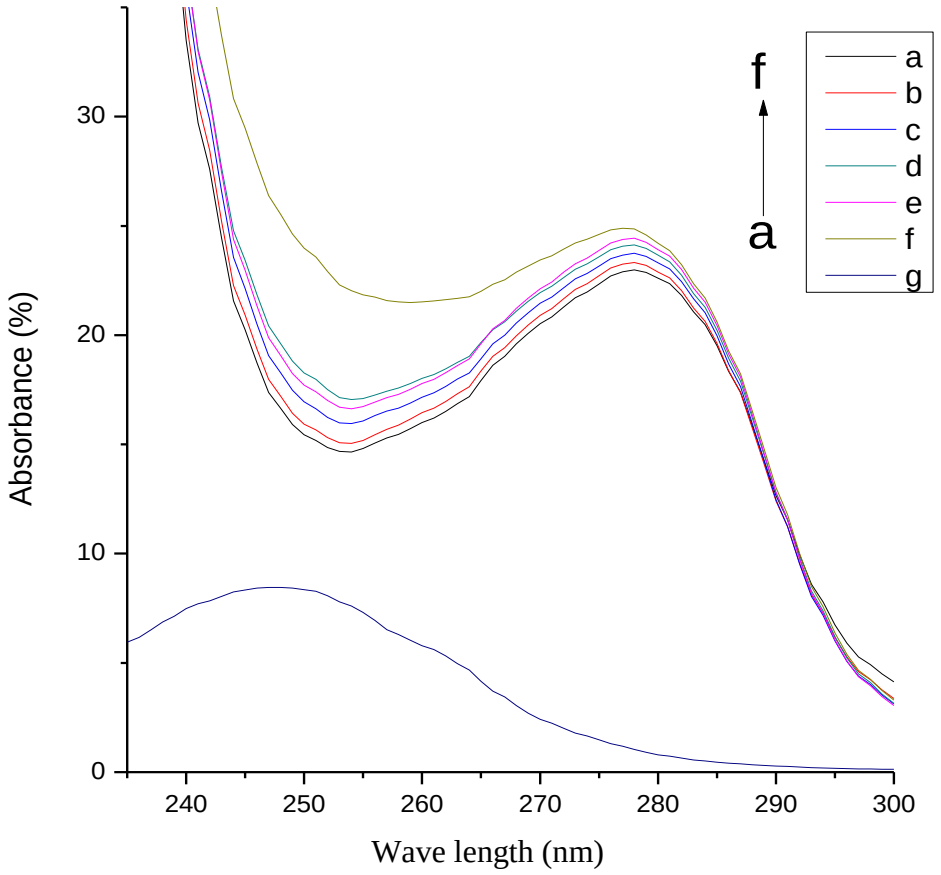

Figure 4.1: UV-absorbance spectra of HSA with different molar ratios of testosterone (a=0:10, b=2:10, c=6:10, d=10:10, e=14:10, f=18:10, g= free testosterone).

The Figure shows the UV-VIS intensity of HSA increases with increasing the testosterone percentage, and the absorption peaks of these solutions showed moderate shifts. This

agrees with past reports that the addition of testosterone extends the peptide strands of HSA molecules more and decreases the hydrophobicity of testosterone (Peng et al. 2008).

The spectrum of the pure hormone showed little or no UV absorption. This result supports the assumption that the peak shifts between free HSA solution and testosterone-HSA complexes are due to the HSA testosterone interactions. Repeated measurements showed consistent results and no significant differences were observed.

4.1.1 Binding constant of testosterone and HSA complexes using UV-VIS Spectrophotometer.

Testosterone–HSA complexes binding constant was determined using UV-VIS spectrophotometer results according to a published method (Stephanos et al. 1996; Koltz et al. 1971; Ouameur et al. 2004) by assuming there is only one type of interaction between testosterone and HSA in aqueous solution, which leads to establish equation (1) and (2) as follows:

HSA + Testosterone $\longleftrightarrow$ Testosterone:HSA

$$K = [\text{ Testosterone:HSA }] / [\text{ Testosterone }][\text{ HSA }] \quad (26)$$

The absorption data were treated using linear double reciprocal plots based on the following equation (Lakowicz 2006) :

$$\frac{1}{A - Ao} = \frac{1}{A\infty - Ao} + \frac{1}{K[A\infty - Ao]} \times \frac{1}{L} \quad (27)$$

A_0 corresponds to the initial absorption of protein at 280 nm in the absence of ligand, A_∞ is the final absorption of the ligated protein, and A is the recorded absorption different testosterone concentrations (L).

The double reciprocal plot of $1/(A-A_0)$ vs. $1/L$ is linear (Figure 4.2) and the binding constant K can be estimated from the ratio of the intercept to the slope to be $(0.349 \times 10^4$ $M^{-1})$ for testosterone-HSA complexes. The value obtained is indicative of a weak testosterone protein interaction with respect to the other drug-HSA complexes with the binding constant in the range of 10^5 and 10^6 M^{-1} (Kargh Hanse 1981) which considered to be the range of strong interaction.

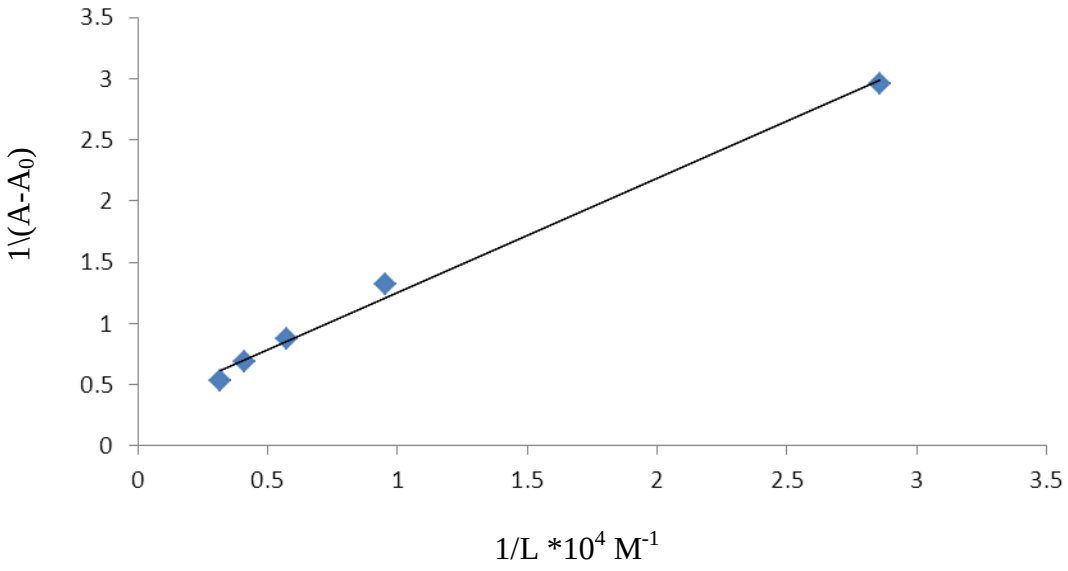

Figure 4.2: The plot of $1/(A-A_0)$ vs 1/L for HSA with different concentrations of testosterone.

4.2 Fluorescence spectrophotometer

Fluorescence spectroscopy can provide information about a wide range of molecular processes, including the interactions of solvent molecules with fluorophores, conformational changes, and binding interactions (Lakowicz 2006).

The intrinsic fluorescence of many proteins is mainly contributed by tryptophan alone, because phenylalanine has very low quantum yield and the fluorescence of tyrosine is almost totally quenched if it is ionized or near an amino group, a carboxyl group, or a tryptophan residue (Darwish et al. 2010).

For HSA-Testosterone complexes excitation wavelength at 360nm was used, and the observed wavelength emission was at 439 nm. The fluorescence sensor was based on intramolecular charge transfer (ICT), which is highly sensitive to the polarity of microenvironment. Therefore, it is expected to act as fluorescent probe for some biochemical systems like proteins (Tian et al. 2003).

The fluorescence quenching spectra of HSA at various percentage of testosterone is shown in Figure 4.3. The fluorescence intensity of HSA gradually decreased while the peak position shows little change when increasing the percentage of testosterone, indicating that it binds to HSA. Under the same condition no fluorescence of testosterone was observed. This indicates the testosterone could quench the auto fluorescence of HSA which means

the interaction between testosterone and HSA occurs, leading to a change in the microenvironment around the tryptophan residue and further exposure of tryptophan residue to the polar solvent (Petitpas et al. 2001; Wang. et al. 2007).

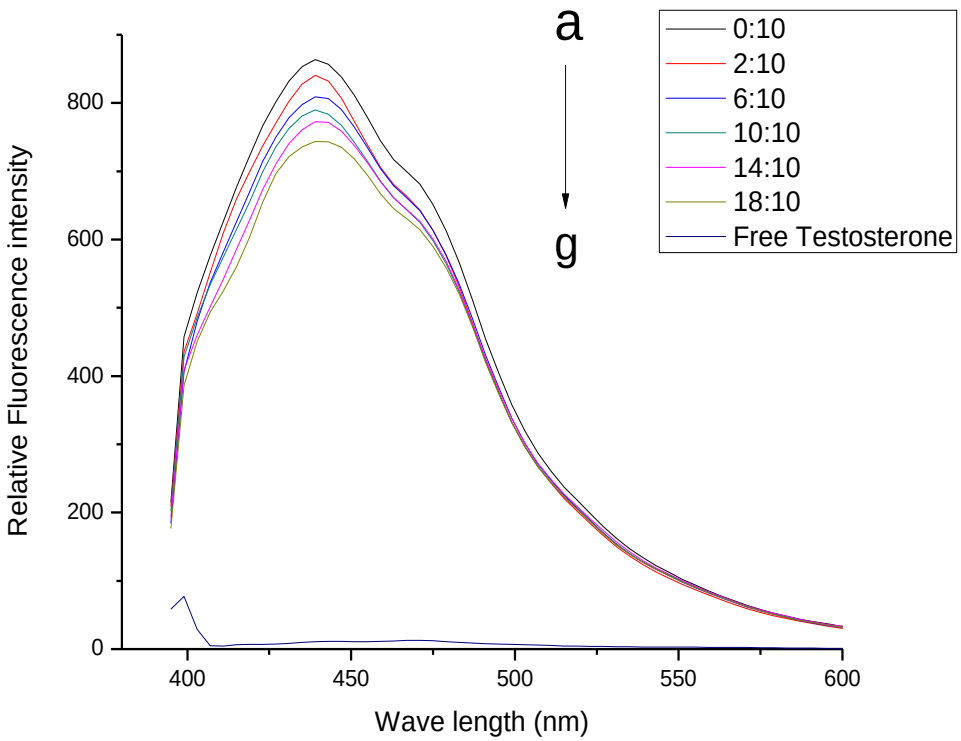

Figure 4.3: Fluorescence emission spectra of HSA in the absence and presence of testosterone in these ratios (T: HSA a=0:10, b=2:10, c=6:10, d=10:10, e=14:10, f=18:10, g=free testosterone).

4.2.1 Stern-Volmer quenching constants (Ksv) and the quenching rate constant of the biomolecule (Kq)

Fluorescence quenching reduces the fluorescence intensity without changing the fluorescence emission spectrum; it can result from transient excited-state interactions (collision quenching) or the formation of non-fluorescent ground-state species.

As discussed in chapter two assuming dynamic quenching dominates the decreased intensity can be described by Stern-Volmer equation:

$$F_0/F = 1+ K_q \tau_0 (L) = 1+ K_{sv}(L) \qquad (28)$$

F and F_0 are the fluorescence intensities with and without quencher, K_{sv} is the Stern-Volmer quenching constant, K_q is the bimolecular quenching constant, τ_0 is the average

lifetime of the biomolecule without quencher, and L is the quencher concentration. K_{sv} values reflect the sensitivity of the fluorophore to a quencher.

Linear curves were plotted according to the Stern-Volmer equation as shown in Figure 4.4 for testosterone-HSA complexes. The quenching constant K_{sv} was obtained from the slope of the curve obtained in Figure 4.4. The value equals (0.0456×10^4 L mol^{-1}).

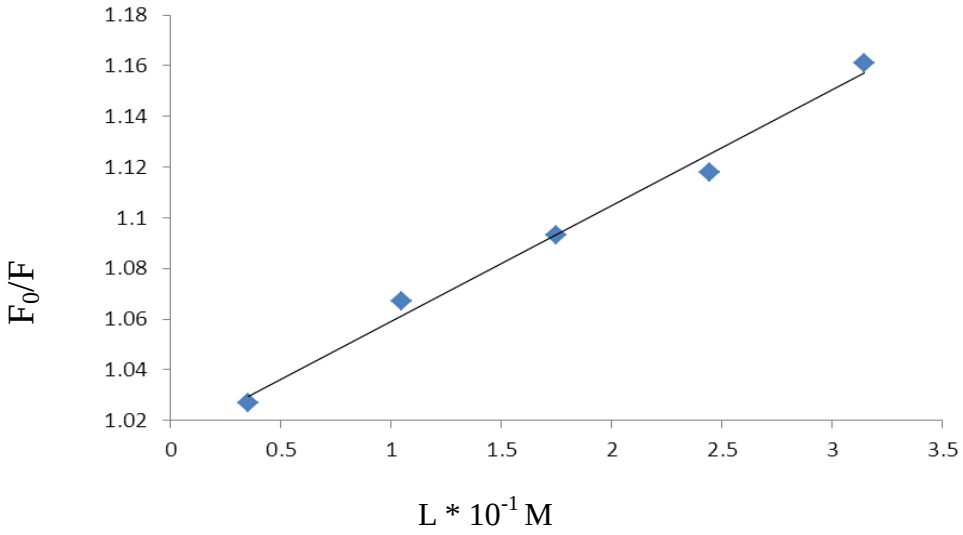

Figure 4.4: The Stern Volmer plot for testosterone –HSA complexes.

From equation 4 the value of $K_{sv} = K_q \tau_0$ from which we can calculate the value of K_q using the fluorescence life time of 10^{-8}s for HSA (Cheng et al). We obtained the K_q values (4.5×10^{10} L $mol^{-1}s^{-1}$). This is larger than the maximum dynamic quenching constant for various quenchers with biopolymer (2×10^{10} L mol^{-1} s^{-1}) (Lakowicz 2006). This may mean the quenching is not initiated by dynamic collision but the formation of a complex resulting in static quenching dominance (Cui et al 2008; Wang et al. 2008).

4.2.2 Determination of the binding constant using fluorescence spectrophotometer.

When static quenching is dominant the modified Stern-Volmer equation could be used (Yang, et al , 1994)

$$\frac{1}{Fo-F} = \frac{1}{FoKL} + \frac{1}{Fo} \qquad (29)$$

K is the binding constant of testosterone-HSA, and can be calculated by plotting 1/ (F_0-F) vs 1/L from Figure 4.5. The obtained value of K is (0.382×10^4) which agrees well with the value obtained earlier UV spectroscopy and supports the effective role of static

quenching. The highly effective quenching constant in this case lowered the value of the hormone- HSA binding constant, due to an effective hydrogen bonding between them (Darwish et al. 2010).

The acting forces between a small molecule and macromolecule include hydrogen bonds, Van der-Waals, electrostatic and hydrophobic interaction forces. It is more likely that hydrophobic and electrostatic interactions were involved in the binding process.

Hydrophobic interaction is mostly an entropic effect originating from the disruption of highly dynamic hydrogen bonds between molecules of liquid water by the nonpolar solutes. Minimizing the number of hydrophobic side chains exposed to water is the principal driving force behind the folding process (Pace C et al 1996). Formation of hydrogen bonds within the protein stabilizes the protein structure (Rose G, et al 2006.

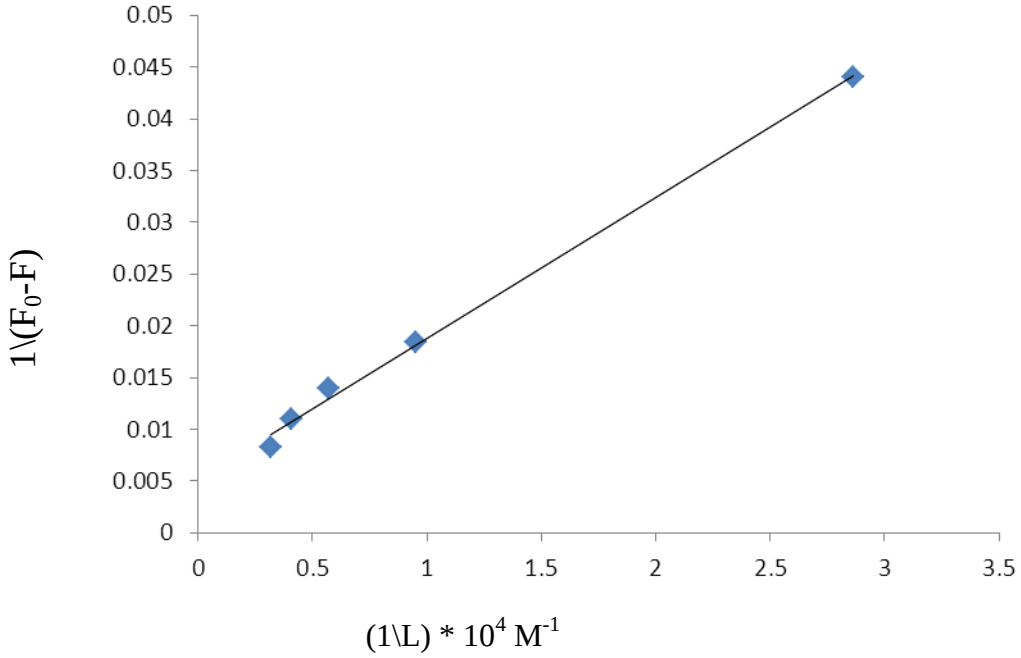

Figure 4.5: The plot of $1/(F_0-F)$ vs $(1/L) \times 10^4$ for testosterone –HSA complexes .

Previous experiment were conducted to investigate the interaction of progesterone and cholesterol with HSA using UV–VIS spectroscopy in addition to investigation of the fluorescence quenching (Abu Teir et al 2010; Abu Teir et al 2012).

We used the same experimental procedures for the Testosterone-HSA bindings. We obtained the binding constant k using UV-VIS spectrophotometer, and the fluorescence spectrophotometer and the Stern-Volmer quenching constant Ksv using UV-VIS spectrophotometer. The values for the two hormones and their parent (cholesterol) are listed in Table 4.1.

Hormone-HSA binding	**Molecular structure**	**Binding constant (UV-VIS)**	**Stern Volmer constant (k_{sv})**	**Binding constant (fluorescence)**
Cholesterol	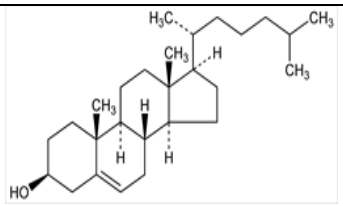	**26.41×10^{2} M^{-1}**	**6.2×10^{2} L Mol^{-1}**	**21.4×10^{2} M^{-1}**
Progesterone	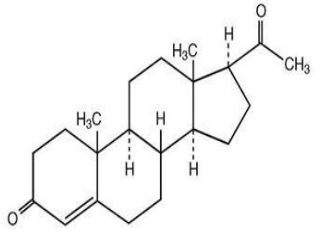	**6.35×10^{2} M^{-1}**	**6.26×10^{2} LMol^{-1}**	**6.56×10^{2} M^{-1}**
Testosterone	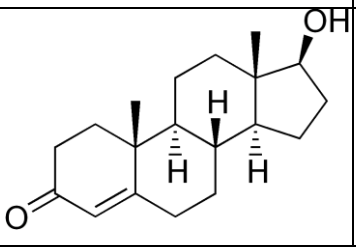	**34.9×10^{2} M^{-1}**	**4.5×10^{2} L Mol^{-1}**	**38.23×10^{2} M^{-1}**

Table 4.1: Testosterone, progesterone and cholesterol comparison.

We can see the testosterone has the highest binding constant of 34.9 - 38.23 $\times10^{2}M^{-1}$ compared to much progesterone (6.35-6.56$\times10^{2}M^{-1}$) and cholesterol (21.4-26.4$\times10^{2}M^{-1}$) (Abu Teir, M. M., et al 2010).

The difference is based on molecular structure variation for the three molecules. The progesterone shows it is a hydrogen bond acceptor, while cholesterol is considered a hydrogen bond donor. The testosterone contains both (OH) and (=O) and it acts like both donor and acceptor.

A pervious study was conducted to investigate the encapsulation capability of a PCL-PEO based block copolymer for hydrophobic drugs with different spatial distributions of hydrogen bond donors and acceptors. Drugs used are classified into two groups. One has multiple hydrogen bond donors and acceptors in their structure while the other contains only clustered hydrogen bond acceptors (Patel, S.K., et al 2010).

We concluded from our study that clustering of H-bonds acceptors restricts their interaction with the PCL blocks in the multi-block architecture and this is not the case for drugs containing evenly distributed H-bond acceptors. This means the presence and distribution of hydrogen donor-acceptor affects the interaction of molecule with other molecule (Patel, S.K., et al 2010).

A similar approach is adopted to explain the difference in quenching and binding constant for testosterone from progesterone and cholesterol. The testosterone as an acceptor-donor molecule has more H-bond sites and it is expected to enhance the formation of hydrogen bonds with the HAS. As for both progesterone and cholesterol the binding probabilities with HSA is expected to be less.

4.3 FT-IR Spectroscopy

FT-IR transform spectrophotometers have greatly extended the capabilities of infrared spectroscopy and are applied to many areas that are very difficult or nearly impossible to analyze by dispersive instruments (Shernan 2014).

FT-IR spectroscopy provides information about secondary content of proteins. This can arise from the amide band which results from the vibrations of the groups around the peptide bonds of proteins (Haris 1999). Changes in the hydrogen bonding involve peptide linkages would occur. This can change the vibrational frequency of the amide modes when the binding between drugs and globular protein like HSA occur.

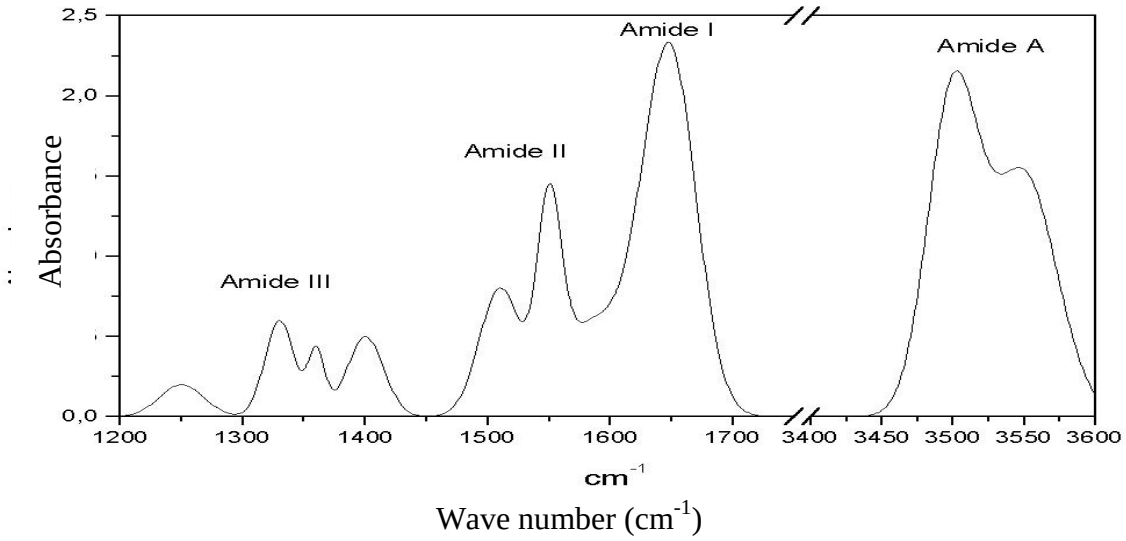

Figure: 4.6: Sample spectrum showing the three relevant regions for determination of protein secondary structure. Amide I (1700-1600 cm^{-1}), amide II (1600-1480 cm^{-1}) , amide III (1330-1220 cm^{-1})

The protein infrared is characterized by a set of absorption the amide regions and the C-H region. The modes most widely used in protein structural studies are amide I, amide II and amide III.

Amide I band range is 1700-1600 cm^{-1} and arises principally from the C=O stretching. Amide II ranges is1600-1480 cm^{-1} and it is primarily N-H bonding with a contribution from C-N stretching vibrations. Amide III band range is 1330-1220 cm^{-1} and it is due to the C-N stretching mode coupled to the in-plane N-H bending mode (Abu Teir, M. M., et al 2010). This mode absorption is normally weak.

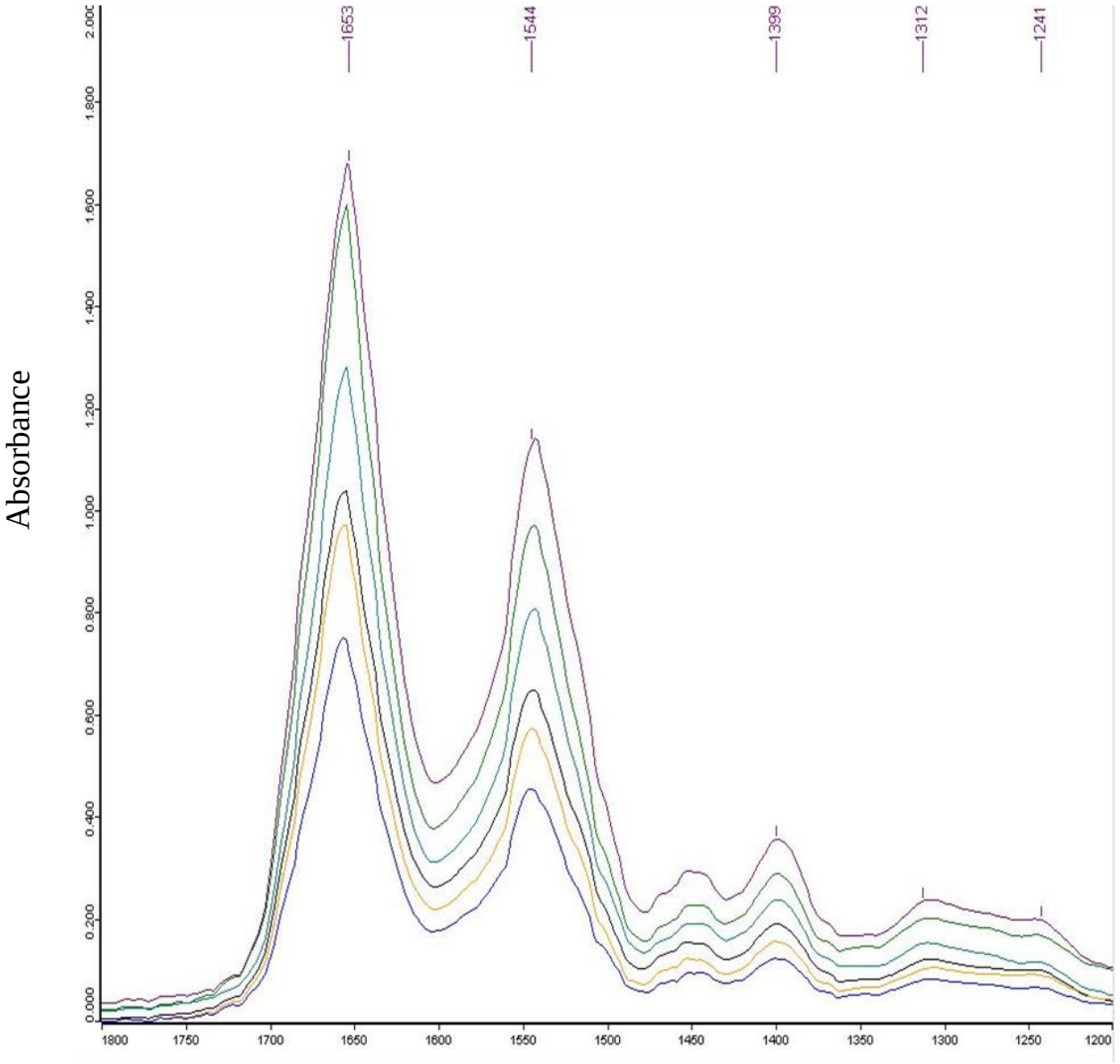

Figure 4.7: The spectrum of Testosterone-HSA complexes with different percentage of testosterone. It is obviously seen as testosterone ratio increases the intensities of the amide I, amide II and amide III bands decreased further in the spectra of all testosterone HSA complexes. The reduction in the intensity of the three amide bands is related to the testosterone HSA interaction.

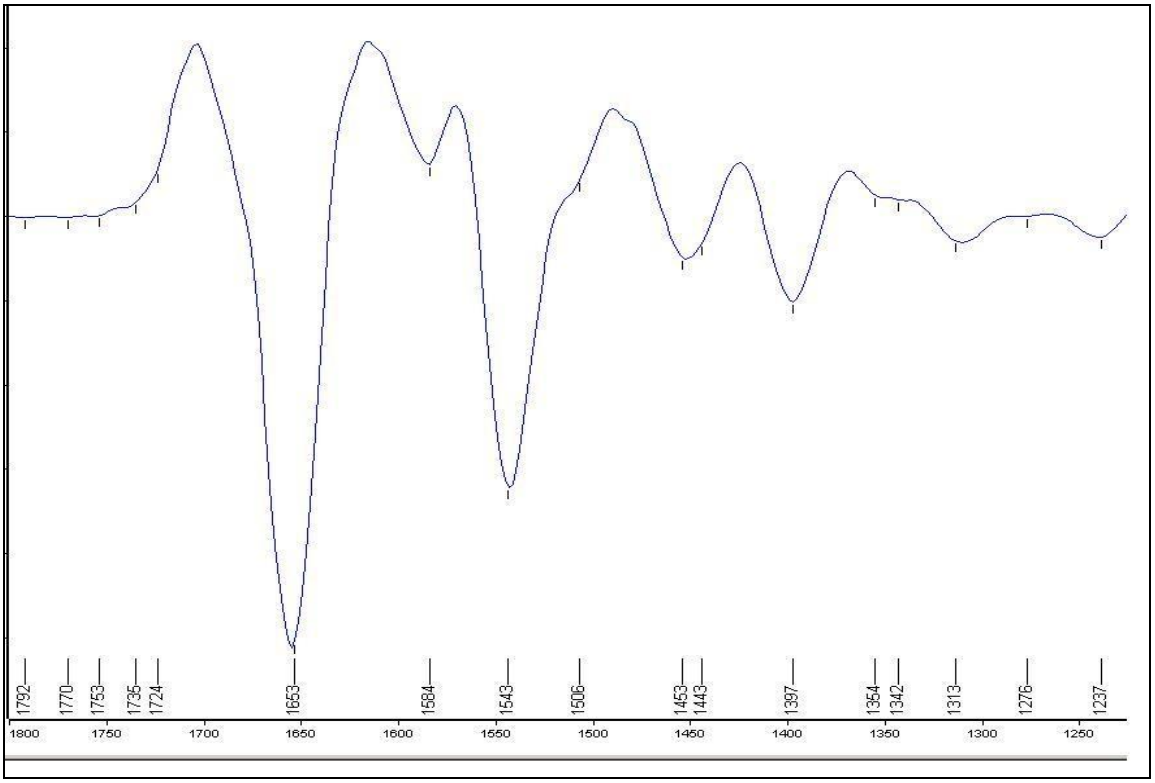

Figure 4.8: The second derivative of free HSA. The spectra are dominated by absorbance bands of amide I and amide II at peak positions 1656 cm-1 and 1545cm-1 respectively.

In Table 4.2 the peak positions of HSA with different ratios of testosterone are listed. For testosterone-HSA the amide bands of HSA infrared spectrum shifted as listed in the table.

For amide I the peak positions have shifted as follows: 1622 cm^{-1} to 1626 cm^{-1}, 1636 cm^{-1} to 1638 cm^{-1}, 1654 cm^{-1} to 1657 cm^{-1}, 1680 cm^{-1} to 1679 cm^{-1} and 1695 cm^{-1} to 1694 cm^{-1} .

For amide II the peak positions have shifted as follows: 1546 cm^{-1} to 1549 cm^{-1} and 1577 cm^{-1} to 1578 cm^{-1}. In addition the new peaks appeared at high molecular ratios of testosterone at 1533 cm^{-1} and 1569.

Bands	HSA Free	T:HSA 2:10	T:HSA 6:10	T:HSA 10:10	T:HSA 14:10	T:HSA 18:10
		1607		1610	1610	
	1622	1622	1622	1624	1625	1626
	1636	1636	1636	1637	1637	1638
Amide I	1654	1655	1655	1656	1657	1657
(1700-1600)	1680	1680	1680	1680	1679	1679
	1695	1695	1695	1695	1694	1694
	1497	1497	1496	1497	1497	1497
	1515	1515	1516	1515	1514	1515
					1533	1533
Amide II	1546	1546	1546	1548	1548	1549
(1600-1480)	1577	1577	1576	1577	1578	1578
					1570	1569
	1594	1594	1594	1594	1594	1594
	1232	1232	1231	1231	1232	1232
	1244	1244	1244	1244	1245	1244
	1267	1267	1267	1267	1266	1267
Amide III	1278	1279				1276
(1330-1220)	1294	1294	1294	1294	1294	1294
	1309	1309	1309	1309	1309	1309
	1325	1325	1325	1325	1325	1325

Table 4.2: Band assignment in the absorbance spectra of HSA with different testosterone molecular ratios for amide I, amide II, and amide III regions.

For amide III the peak positions are also have been shifted as the follows: 1278 cm^{-1} to 1276 cm^{-1}.

Change in the peak shape for certain elements can occur due to the difference in the chemical bonding, between samples and standards. The peaks shape change of HSA after interaction with testosterone occurred due to the changes in protein secondary structure. Those changes are attributed to the imposed hydrogen bonds between testosterone (on both =O and –OH sites) and the protein (Sarver & Krueger 1991).

For the testosterone-HSA amide I band, we observed a shift to higher frequency for the second peak (1622-1626 cm^{-1}) and the major peak (1654-1657 cm^{-1}). In amide II the largest shift occurred at the major peak (1546-1549 cm^{-1}). Only one shift in amide III occurred at (1278-1276 cm^{-1}), and it was not observed for all samples.

Hydrogen bonding can affect the bond strength that causes the peak shift, In made I the observed characteristic band shifts often allow the assignment of these bands to peptide groups or to specific amino-acid side-chains.

An additional advantage is the shift of the strong water absorbance away from the amide I region (1610–1700 cm^{-1}) which is sensitive to protein structure. The minor but reproducible shift indicates that a partial unfolding of the protein occurs in HSA, with the retention of a residual native-like structure. The peaks shifts tend to move towards a higher wave number, this implies an increase in the bond strength but with a small percentage (Uversky 2007).

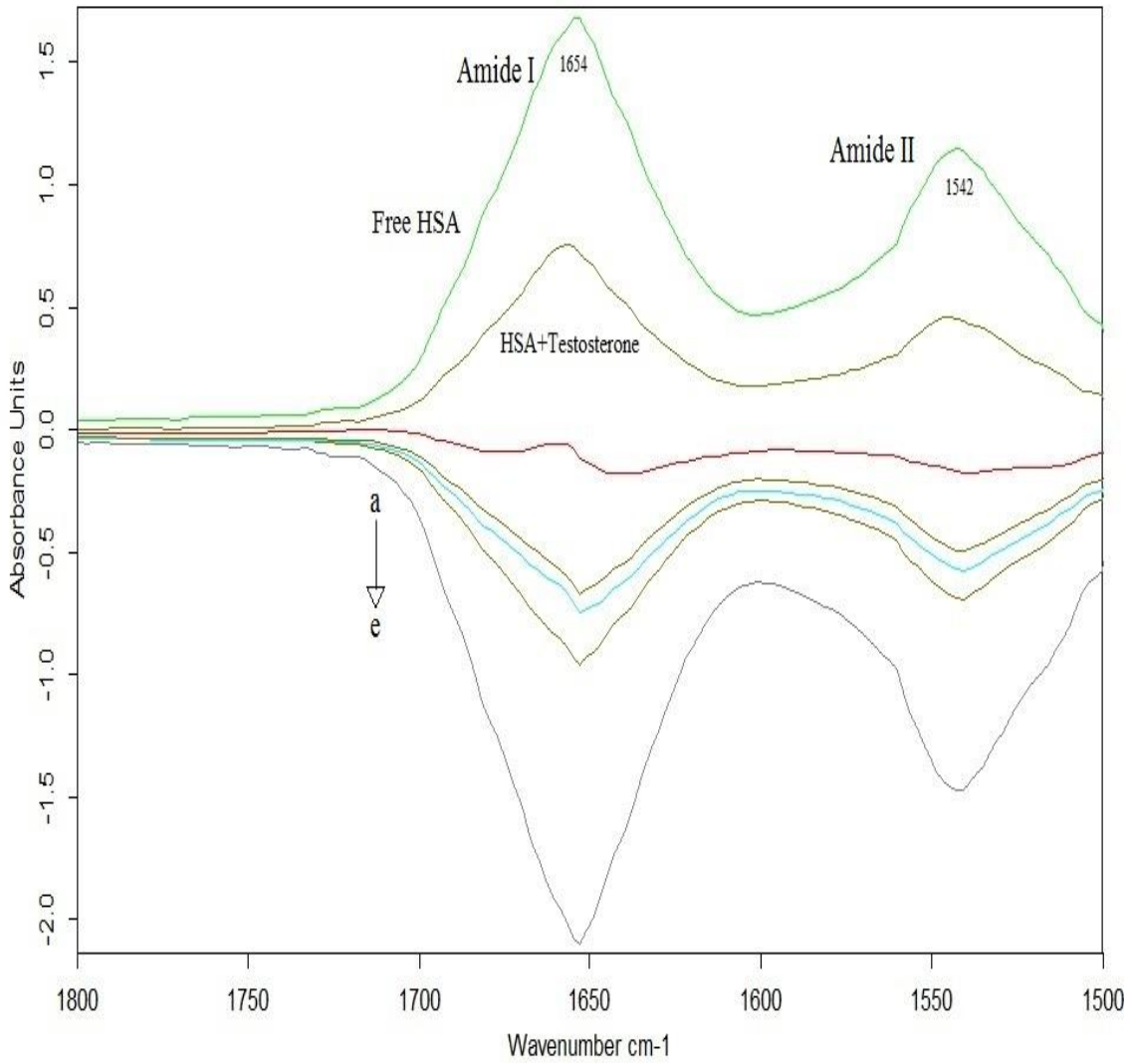

Figure 4.9: FT-IR spectra (top two curves) and difference spectra (from a to e) of HSA and its complexes with different testosterone concentrations in the region 1800-1500 cm-1. (a= Diff (T+HSA) [2:10], b=Diff (T+HSA) [6:10], c= Diff (T+HSA) [10:10], d= Diff T+HSA [14:10], e= Diff T+HSA [18:10]).

The difference spectra for [(HSA+Testosterone) – (Free HSA)] were obtained to monitor the intensity variations of these vibrations. The results are shown in Figures 4.9-4.10. Figure 4.9 shows FT-IR spectra (two top curves) and difference spectra of HSA compounds with different testosterone percentages for amide I and II regions. Figure 4.10 shows the difference spectra of HSA compounds with different testosterone percentage for amide III region.

In amide I a strong negative feature appears at 1654 cm^{-1}. Another negative feature appears at 1542 cm^{-1} for in amide II. For amide III two negative features appear at 1308 $cm^{-1}$and 1245 cm^{-1} with a little change as testosterone ratios were increased.

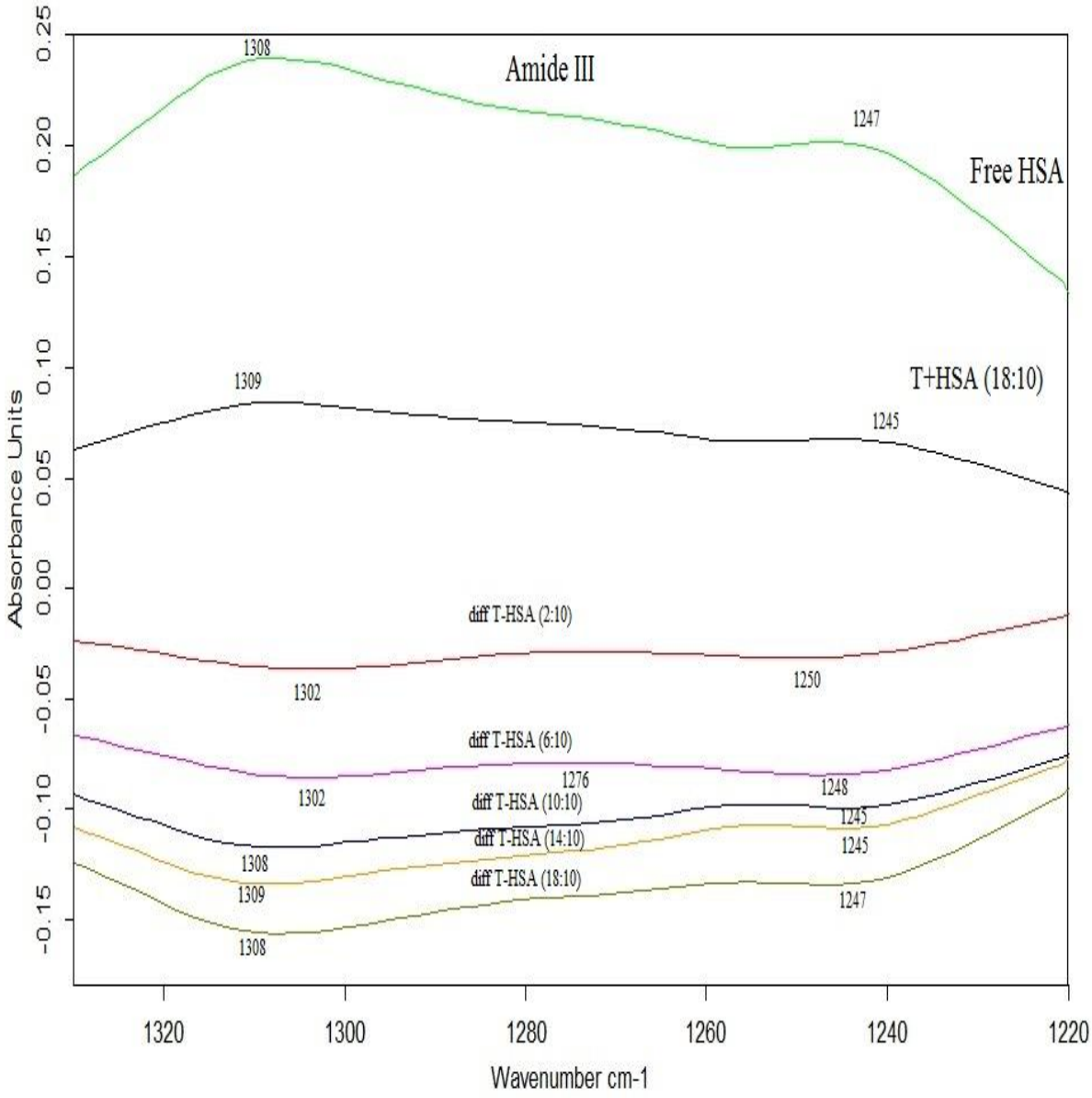

Figure 4.10: FT-IR spectra (top two curves) and difference spectra of HSA and its complexes with different testosterone concentrations in the region of 1330-1220 cm^{-1}.

The strong negative features of the difference spectra become stronger as the percentage of testosterone was increased with a little shift in their positions. This is are attributed to the intensity decrease in the amide I, II and III bands in the spectra of the testosterone-HSA and the interaction (H-bonding) of the testosterone with protein C=O and C-N groups, and the reduction of the proteins α-helix structure upon interaction (Purcell et al. 2000; Krimm et al.1986)

The shape of the amide I band of globular proteins is characteristic of their secondary structure Byler & Susi. The determination of secondary structures in proteins from FT-IR

spectra is now possible due to the availability of high signal to noise ratio digitalized spectra obtained by FT-IR spectrometer.

To obtain a quantitative analysis of the protein secondary structure forming HAS, the basic analytical tools used are the infrared Fourier Self Deconvolution in addition to curve fit and second derivative resolution.

The aim of Fourier Self-Deconvolution (FSD) is to enhance the resolution of a spectrum, or decrease the line width. Spectral ranges comprising broad and overlapping lines can thus be separated into sharp single lines. FSD is only useful in the case when the lines are substantially broader than the spectral resolution (OPUS Bruker manual version 5.5, 2004). Amide I, amide II and amide III regions were assigned to secondary structures according to the frequency of its maximum a raised after Fourier self deconvolution has been applied.
Amide I 1610- 1700 cm^{-1} was divided as follows: 1610-1624 cm^{-1} representing β-sheets, 1625-1640 cm^{-1} random coil, 1646-1671 cm^{-1} α-helix, 1672-1787 cm^{-1} turn structure, and 1689-1700 cm^{-1} to antiparallel β- sheets.

Amide II 1480-1600 cm^{-1} was divided as follows: 1488-1504 cm^{-1} to β-sheet, 1508-1523 cm^{-1} to random coil, 1528-1560 cm^{-1} to α-helix, 1562-1585 cm^{-1} to turn structure, and 1585-1598 cm^{-1} to antiparallel β- sheets.

Amide III 1220-1330 cm^{-1} was divided as follows: 1220-1256 cm^{-1} to β-sheet, 1257-1285 cm^{-1} to random coil, 1287-1301 cm^{-1} to turn structure, and 1302-1329 cm^{-1} to α-helix.

The investigation in amide I absorption was primarily determined by the backbone conformation and independent of amino acid sequence (Krimm, S & Bandekar, J 1986).

For amide II and III band more information can be gained as various types of chemical bonds are involved and that can be useful in predicting the protein secondary structure.

2nd Structure	HSA free (%)	HSA-T 2:10 (%)	HSA-T 6:10 (%)	HSA-T 10:10 (%)	HSA-T 14:10 (%)	HSA-T 18:10 (%)
Amide I						
β-sheets (cm^{-2}) (1610-1624) (1689-1700)	**17**	**19**	**20**	**21**	**22**	**22**
Random (cm^{-2}) (1625-1640)	**10**	**10**	**10**	**10**	**9**	**8**
α-hilex (cm^{-2}) (1646-1669)	**63**	**62**	**59**	**58**	**59**	**57**
Turn (cm^{-2}) (1672-1687)	**10**	**9**	**11**	**11**	**11**	**13**
Amide II						
β-sheets (cm^{-2}) (1488-1504) (1585-1598)	**31**	**34**	**35**	**34**	**35**	**37**
Random (cm^{-2}) (1508-1523)	**9**	**7**	**7**	**8**	**7**	**6**
α-hilex (cm^{-2}) (1528-1560)	**49**	**47**	**46**	**46**	**44**	**44**
Turn (cm^{-2}) (1562-1585)	**11**	**12**	**12**	**12**	**13**	**13**
Amide III						
β-sheets (cm^{-2}) (1220-1256)	**34**	**38**	**43**	**46**	**47**	**52**
Random (cm^{-2}) (1257-1285)	**12**	**11**	**11**	**7**	**7**	**8**
α-hilex (cm^{-2}) (1302-1329)	**50**	**47**	**42**	**41**	**41**	**35**
Turn (cm^{-2}) (1287-1301)	**4**	**4**	**4**	**6**	**5**	**5**

Table 4.3: Secondary structure determination for Amide I, amide II, and amide III regions in HSA and its testosterone complexes.

Based on the above assignments, the percentages of each secondary structure of HSA were calculated by integrating the areas of the component bands in amide I, II and III then divided by the total area. The result is taken as the proportion of the polypeptide chain in that conformation.

The secondary structure determination for the free HSA and its testosterone compounds are given in Table 4.3. It shows the content of each secondary structure of HSA before and after the interaction with testosterone at different ratios. It is seen that α-helix percentage decreases with the increase of testosterone ratios in the calculations. This trend is consistent for the three amide regions.

The second derivative resolution enhancement and curve-fitted amide I, II and III regions and secondary structure determinations of the free HSA and its testosterone compounds (T-HSA 18:10) with the highest of testosterone in dehydrated films are shown in figures (4.11 to 4.16).

For testosterone- HSA interaction:

For amide I: HSA free consisted of 17% β-sheet, 10% random coil, 63% α-helical structure, and 10% turn structure. After testosterone HSA complexation, α-helical structure decreased from 63% to 57%, β-sheets increased from 17% to 22%, turn structure increased from 10% to 13% and random coil decreased from 10% to 8%. (see Table 4.3 and Figures 4.11, 4.12).

For amide II: HSA free consisted of, 31%β-sheets, 9%random coil, 49% α-helical structure, and 11% turn structure. After testosterone –HSA interaction, α-helical structure reduced from 49% to 44%, β-sheets increased from 31% to 37%, random coils decreased from 9% to 6% while turn structure increased from 11% to 13%.

For amide III HSA free consisted 34% β-sheet, 12% random coil, 50% α-helical structure and 4% turn structure. After testosterone-HSA interaction, α-helical structure decreased from 50% to 35%, β-sheet increased from 34% to 52%, random coil decreased from 12% to 8% and turn structure increased from 4% to 5%.

The decrease of the α-helix percentage with the increase of testosterone concentration is evident and this trend is consistent for the three Amide regions. For the β-sheet the relative percentage increased with the increase of testosterone concentration.

The decrease of α-helix intensity percentage in contrast to the increase of β-sheets is believed to be due to the unfolding of the protein in the presence of testosterone as a result of the formation of H bonds between HSA and the hormone.

The newly formed H-bonds result in the C-N bond assuming partial double bond character due to a flow of electrons from the C=O to the C-N bond which decreases the intensity of the original vibrations. This consistent with past work (Krim et al. 1986; Jackson 1991) .

The hydrogen bonds in α-helix are formed outside the helix (the amino-acid side-chains are on the outside of the helix) and parallel to the helix axis, while for β-sheet the hydrogen bonds take position in the planes of β-sheets as the preferred orientations especially in the antiparallel sheets.

The restrictions on the formation of hydrogen bonds in β-sheet compared to α-helix explains the contrasting behaviors Conformational transitions from an α-helix to β-sheet structure were observed for protein unfolding upon protonation and heat denaturation (Surewicz et al. 1987; Holzbaur et al. 1996).

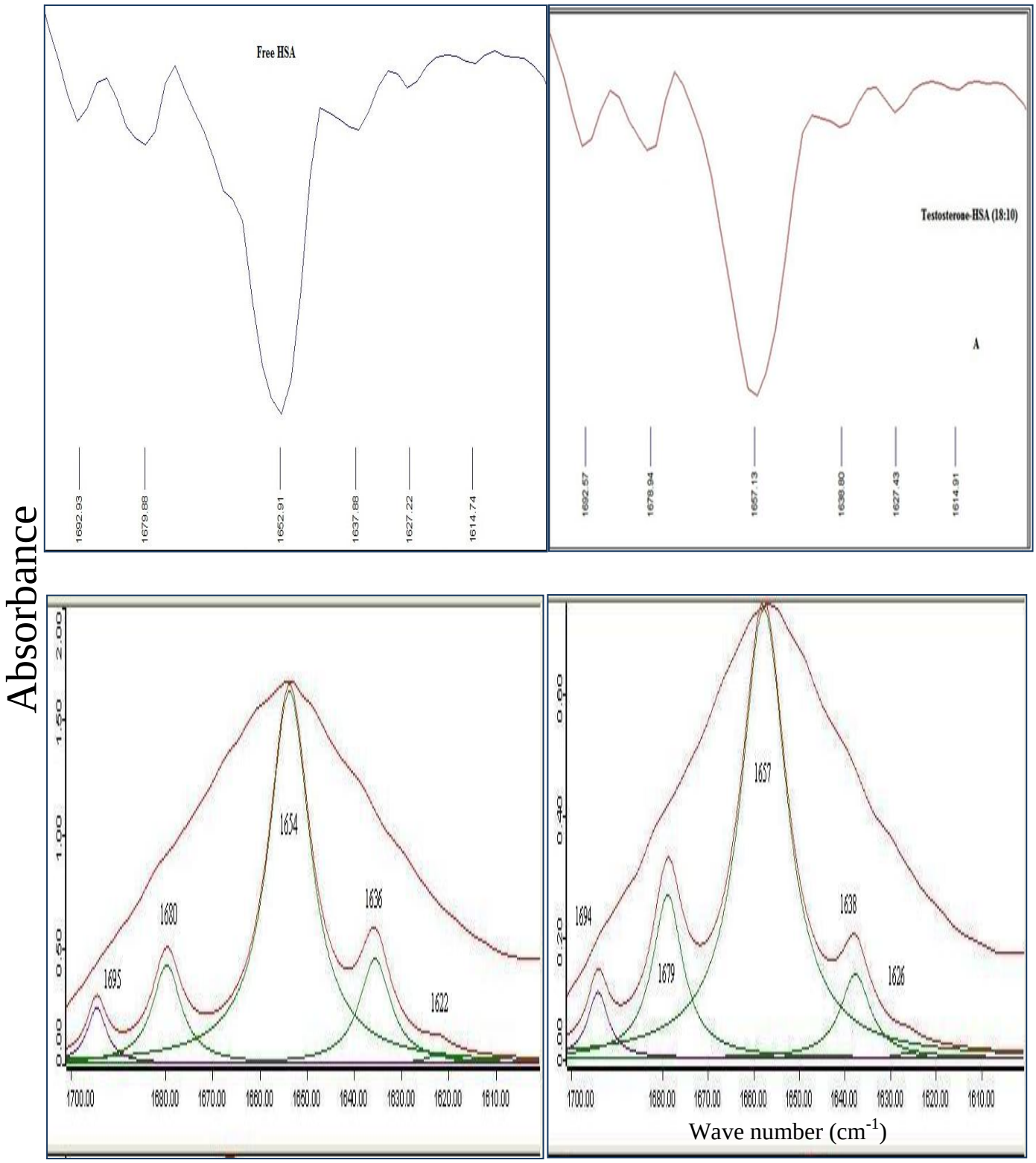

Figure 4.11: Second derivative enhancement and curve fitted Amide I region (1610-1700 cm^{-1}) and secondary structure determination of the free human serum albumin.

Figure 4.12: Second derivative enhancement and curve fitted Amide I region (1610-1700 cm^{-1}) and secondary structure determination of human serum albumin and its testosterone complexes with 18:10 testosterone:HSA ratio.

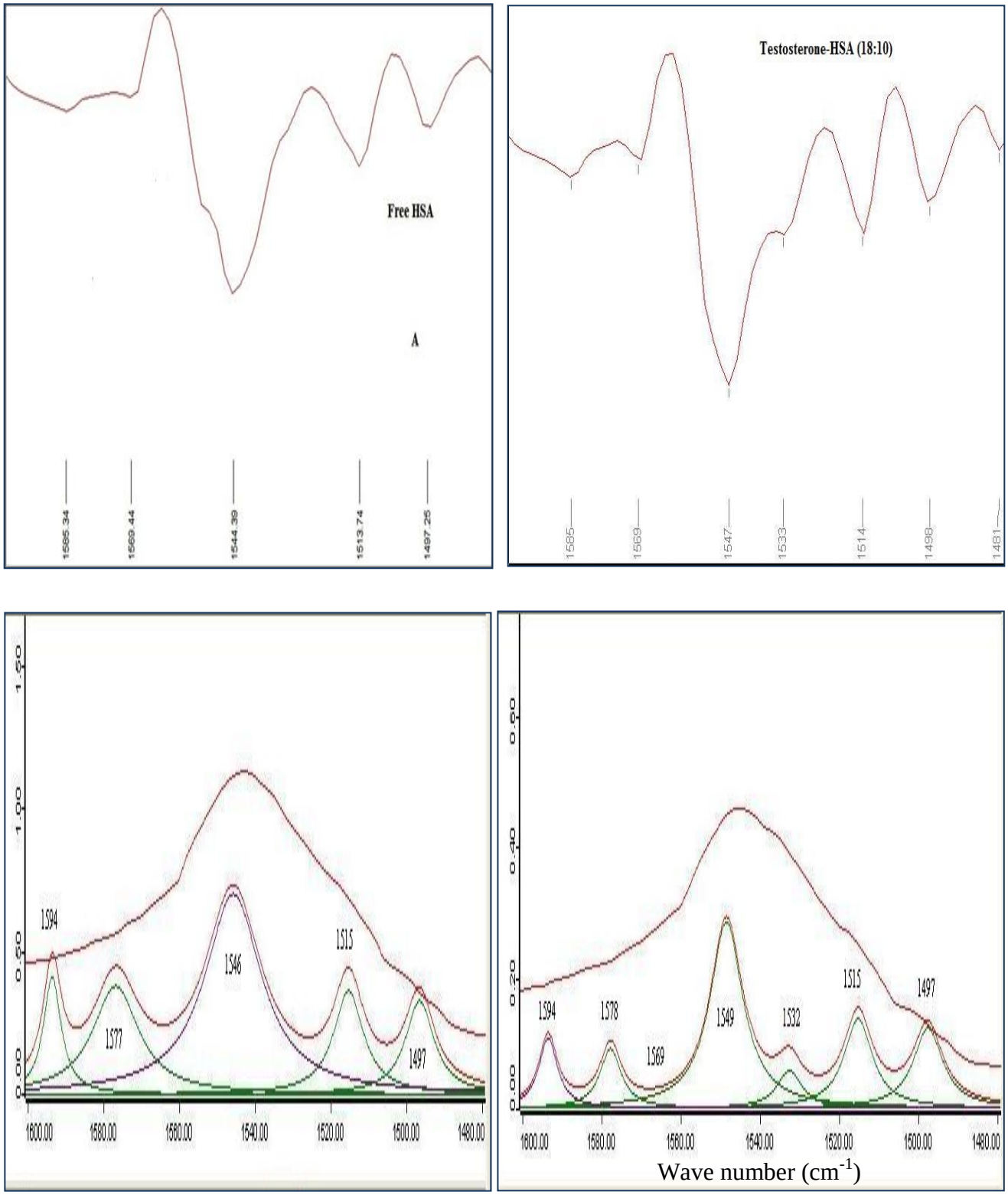

Figure 4.13: Second derivative enhancement and curve fitted amide II region (1600-1480 cm^{-1}) and secondary structure determination of the free human serum albumin.

Figure 4.14: Second derivative enhancement and curve fitted Amide II region (1600-1480 cm^{-1}) and secondary structure determination of t human serum albumin and its testosterone complexes with 18:10 testosterone:HSA ratio.

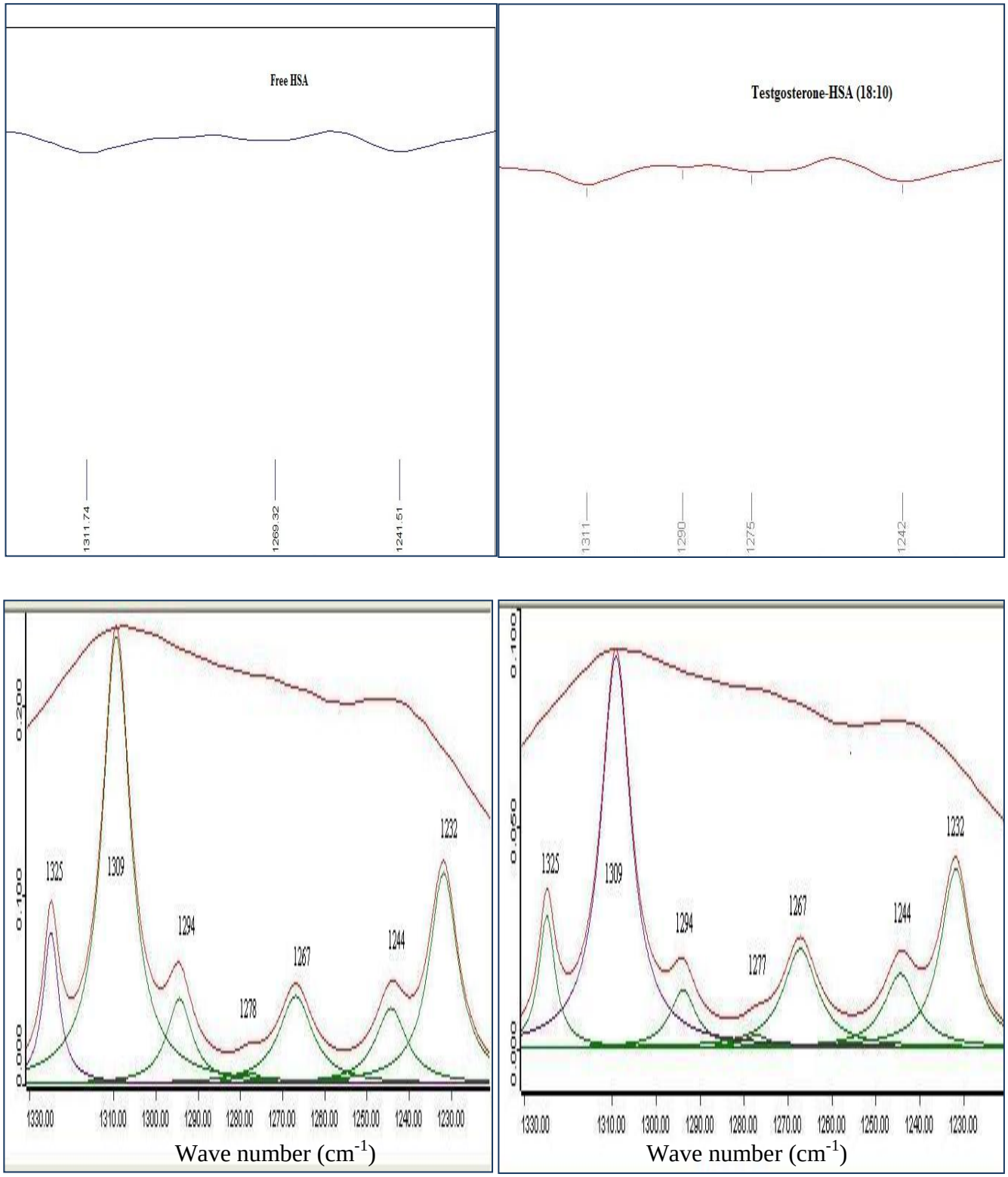

Figure 4.15: Second derivative enhancement and curve fitted amide III region (1330-1220 cm^{-1}) and secondary structure determination of the free human serum albumin. complexes with 18:10 testosterone:HSA ratio.

Figure 4.16: Second derivative enhancement and curve fitted Amide III region (1330-1220 cm^{-1}) and secondary structure determination of human serum albumin and its testosterone complexes with 18:10 testosterone:HSA ratio.

Chapter Five

Conclusions and future work

Chapter five

Conclusions and future work

The interaction between testosterone (male hormone) and HSA Albumin (the universal hydrophobic molecule carrier) was investigated using spectroscopic techniques including (FT-IR, Fluorescence and UV-VIS spectrophotometers). Our experimental work showed relatively high binding affinity between testosterone and HSA.

Using the UV spectrum the calculated binding constant for testosterone-HSA was K= 34.9×10^{2} M^{-1}. The analysis of fluorescence spectrum yielded the binding constant for testosterone-HSA interaction to be K=38.23×10^{2} M^{-1}.The binding constant obtained by different methods has close values. Comparing the binding constant for testosterone with the previously measured binding constants of cholesterol and progesterone (26.4×10^{2} M^{-1}, 6.354×10^{2} M^{-1} respectively) one can conclude that testosterone-HSA interaction is the strongest as it is considered to be both hydrogen donor and acceptor.

Cholesterol interaction with albumin was substantially weaker than testosterone-HSA interaction but stronger than progesterone-HSA interaction. The measured values of Stern-Volmer quenching constant K_{sv} and the quenching rate constant K_q for testosterone were K_{sv}= 4.5×10^{2} L Mol^{-1} and K_q= 4.5×10^{10} $LMol^{-1}s^{-1}$ comparing to values which have been calculated for cholesterol and progesterone respectively (K_{sv} 6.2×10^{2} L Mol^{-1}, K_{sv} 6.26×10^{2} L Mol^{-1}). These results indicate that the static quenching is responsible for the fluorescence quenching (decrease of intensity) which is an indication of complex protein and hormone formations.

Our analysis of FT-IR spectrum indicates that increasing the concentration of testosterone leads to protein unfolding and a reduction of α-helical structure percentage in favor of β-sheet structure (Uversky 2007).

We observed that HSA-Testosterone complexes shifted the peaks of HSA. This is due to a change in the bond strength and partial unfolding of the protein. The newly imposed hydrogen bonds result in the C-N bond assuming partial double bond character due to the flow of electrons from the C=O to the C-N bond which decreases the intensity of the original vibrations (Sarver & Krueger 1991).

Previous studies reported that tyrosine absorbs strongly at 1515 cm^{-1}, and a band at this frequency was found in a number of proteins and assigned to the tyrosine residue (Bendit 1967, Barth 2000). In addition it was reported that the Tyrosine band shifts are due to the altered hydrogen bonding or changes in the $\pi-\pi$ interactions and that indicates alterations in the local environment of the Tyrosine side-chain (Barth 2000).

Our results indicate that there is almost no shift in tyrosine absorption, this can be considered as an indication that testosterone interaction does not affect tyrosine residue. We can consider it as an internal control for the protein mico-environment change.

Another study reported that Tyrosine-OH group interacts with the protein backbone by hydrogen bonding than constitutively absorbs at 1594 cm^{-1} which remained constant in our results. This may indicate that the testosterone interaction with HSA does not affect the hydrogen bonding between R group of the Tyrosine and the backbone of the protein (Barth 2000).

These measurements are important for the field of drug design, and can shed light about changes occurring to the HSA structure resulting from the interaction with testosterone. This can be utilized for diagnostic purposes.
In case of testosterone concentration abnormality regardless of its source (natural or of anabolic testosterone), studying testosterone-HSA interaction and how it affects the protein structure may help in predicting their existence or the hormones disorders by comparing the normal and high concentration testosterone cases.

HSA affinity to bind with other molecules and drugs may be affected by increasing Testosterone-HSA binding affinity. This may cause a shortage of supplying the target tissues with certain molecules in addition to effecting the efficiency of some drugs as HSA may tend to bind with testosterone more than other substances.

Further investigations are recommended in relation to temperature effects on testosterone-Human serum interactions, and how does the protein structure varies with temperature.

References

- Abu Teir M. M., Ghithan J., Abu-Taha M. I.1, Darwish S. M., Abu-hadid M. M..(2014). Journal of Biophysics and Structural Biology. 6(1).1-12.
- Abu Teir, M. M., Ghithan, J. H., Darwish, S. M., Abu-Hadid, M. M..(2010). Journal of Applied Biological Sciences. 4 (3). p79-92.
- Abu Teir, M. M., Ghithan, J., Darwich, S., Abu-hadid, M. M. (2012). Journal of Applied Biological Science. 6 (3), P45-55.
- Anderson. D. C. (1974). Sex Hormone Binding Globulin. Clinical Endocrinology 3, p 69-96.
- Azimi,O.,Emami,Z.,Salari,H.,Chamani,J..(2011).Molecules.www.mdpi.com/journal/molecules.
- Banwell, C. N. (1972): Fundamentals of Molecular Spectroscopy. 2nd ed., McGRAW- HILL Bokk Company (UK) Limited.
- Barth, A. (2000). The infrared absorption of amino acid side chains. Progress in Biophysics & Molecular Biology. 74 (2000) 141-173.
- Bendit, E. G. (1967). Infrared absorption of Tyrosine side chains in proteins. Biopolymers. Volume 5, Issue 6, P 525-533, June 1967.
- Bhattacharya, A., Gruene, T., Curry, S. (2000). Crystallographic Analysis Reveals Common Modes of Binding of Medium and Long-chain Fatty Acids to Human Serum Albumin. J. Mol. Biol, 303, P 721-732).
- Brandt S. F. (1999). Introduction to Steroid Hormones. http://www.rosehulman.edu/~brandt/Chem330/EndocrineNotes/Chapter_1_Steroids.pdf
- Bridgewater State College, Frank R. Gorga: Introduction to Protein Structure. http://webhost.bridgew.edu/fgorga/proteins/.
- Carter, Xiao-MinHe, Sibyl H. Munson, Pamela D. Twigg, Kim M., Gernert, M. Beth Broom, Teresa, Y. Miller (1989) .Three-Dimensional Structure of Human Serum. The Space Science Laboratory, ES76 Biophysics, Marshall Space Flight Center, USA. Daniel C.
- Cheng, F. Q., Wang, Y. P., Li, Z.P., Chuan, D. (2006). Spectrochimica Acta Part A, 65, p144.
- Coleman, P.B. (1993). Practical Sampling Techniques for Infrared Analysis. CRC press LLC .
- Colin, D. (2014): Introduction to Protein Structure Prediction. www.bioststst.wisc.edu/bmi776/
- Cooper, A. (2004). Biophysical Chemistry, The Royal Society of Chemistry, UK.
- Cox RM, John-Alder HB (December 2005). "Testosterone has opposite effects on male growth in lizards (Sceloporus spp.) with opposite patterns of sexual size dimorphism". J. Exp. Biol. 208 (Pt 24): 4679–87.
- Cui, F., Wang, J., Li, F., Fan, J., Qu, G., Yao, X., Lei, B. (2008). Chinese Journal of Chemistry, 26, p661.
- Cui, A., Lixia Qin, A., Guisheng, Z. A., Xiaobing, L.A., Xiaojun, Y. B., Beilei ,L. B . (2008). A concise approach to 1,11-didechloro-6-methyl-40-O-demethyl rebeccamycin and its binding to

human serum albumin: Fluorescence spectroscopy and molecular modeling method Fengling. Bioorganic & Medicinal Chemistry,16,7615–7621.

- Darwish, S. M., Abu Sharkh, S. E., Abu Teir, M. M., Makharza, S. A., Abu-hadid, M. M. (2010). Journal of Molecular Structure, 963, p122–129.
- Derrick, M.R., Stulik, D., Landry, J.M.. (1999): Infrared Spectroscopy in Conservation Science. The Getty Conservation Institue, Los Angelos.
- Dewey, Colin: Introduction to Protein Structure Prediction. www.biostst.wisc.edu/bmi776/
- Dong, C.Y., So, P.T.. (2002). Fluorescence Spectrophotometry. Massachusetts Institute of Technology, Macmillan Publishers Ltd.
- Duke University, Richardson, Jane. S.: The Anatomy and Taxonomy of Protein Structure. http://kinemage.biochem.duke.edu/teaching/anatax/index.html
- Dukor , R.K., Chalmers, J.M., Griffiths, P.R. (2001): Vibrational Spectroscopy in the Detection of Cancer, Handbook of Vibrational Spectroscopy, Vol.5, John Wiley and Sons, Chichester.
- Fabian, H., Schultz, C., Backman, J., Hahn, U., Saenger, W., Mantsch, H. H., Naumann, D. (1994). Biochemistry, 33 , p 10725.
- Frye CA (2009). "Steroids, reproductive endocrine function, and affect. A review". Minerva Ginecol 61 (6): 541–562. PMID 19942840.
- Goormaghtigh, E., Ruysschaert, J.M., Raussens, V. (2006). Biophysical Journal, 90. P 2946.
- Gordon G. Allison (2011). Application of Fourier Transform Mid-Infrared Spectroscopy (FT-IR) for Research into Biomass Feed-Stocks, Fourier Transforms - New Analytical Approaches and FT-IR Strategies, Prof. Goran Nikolic (Ed.), ISBN: 978-953-307-232-6, InTech, Available from: http://www.intechopen.com/books/fouriertransforms-new-analytical-approaches-and-FT-IR-strategies/application-of-fourier-transform-mid-infraredspectroscopy-FT-IR-forresearch-into-biomass-feed-stock.
- Gorga, F.R.(2007): Introduction to Protein Structure. Bridgewater State College. http://webhost.bridgew.edu/fgorga/proteins/
- Griffiths, P.R., de Haseth, J.A.(2007): Fourier Transform Infrared Spectroscopy, 2nd, John Wiley & Sons, New Jersey.
- Groper, S. S., Smith, J. L., Groff, J. L. (2009): Advanced Nutrition and Human Metabolism. 5th ed. Canada: Wadsworth Cengage Learning.
- Gudrun,J., Mareike, M., Patrick, G., Michel H.J. Koch3, Hiroshi,N., Alfred, B., Klaus ,B. (2002). Investigation into the interaction of recombinant human serum albumin with Re-lipo-polysaccharide and lipid .Journal of Endotoxin Research 2002; 8; 115
- Hardie , D.G. (1991): Biochemical Messengers, Hormones, Neurotransmitter and Growth Factors, 1st , University Press, Cambridge.
- Haris , P. I., Severcan, F. (1999). Journal of Molecular Catalysis B: Enzymatic, 7 , P 207.

- Hildebrandt, P., Siebert, F (2008): Vibrational Spectroscopy in Life Science, 1st, John Wiley & Sons Ltd, UK.
- Hollas, J. M (2004): Modern spectroscopy, 4th, John Wiley & Sons Ltd, UK.
- Hornaback, J.M. (2006): Organic Chemistry,2nd, Thomson learning, Inc, Madrid, Spain.
- Hsieh, H.N. (2008): FT-IR lab instruction, New Jersey Institute of Technology: http://www-ec.njit.edu/~hsieh/ene669/FT-IR.html
- II'ichev, Y.V., Perry, J.L., Simon, J.D. (2002). J. Phys. Chem. B, 106, P460.
- International Union of Pure and Applied Chemistry. Compendium of Chemical Terminology "Goldbook". Version 2.3.2. 2012.
- IUPAC, Compendium of Chemical Terminology, 2nd ed. (the "Gold Book") (1997). Online corrected version: (2006–) "hydrophobic interaction".
- Jackson, M., Mantsch, H.H. (1991). J.Chem., 69, p 1639.
- Ji-Sook, Ha.A., Theriault,A.C., Nadhipuram,V., Bhagavan A., Chung-Eun Ha.B.. (2006). Fatty acids bound to human serum albumin and its structural variants modulate apolipoprotein B secretion in HepG2 cells. Biochimica et Biophysica Acta 1761 (2006) 717–724)
- Johnson. L., Spence. T. Z. M.. (2010). Fundamental of fluorescence. Molecular Probes Handbook, A Guide to Fluorescent Probes and Labeling Technologies.11th ed.
- Kandagal, P. B., Shaikh, S. M. T., Manjunatha, D. H., Seetharamappa, J., Nagaralli, B.S.(2007). Spectroscopic studies on the binding of bioactive phenothiazine compounds to human serum albumin. J. Photochem. Photobiol. A 189, P 121-127.
- Kang, J., Liu, Y., Xie, M.X., Li, S., Jiang, M., Wang, Y.D. (2004). Interactions of human serum albumin with chlorogenic acid and ferulic acid. Biochimica et Biophysica Acta ,1674, P 205–214.
- Kargh-Hanse, U.(1981). Pharmacol. Rev., 33 , p17.
- Klotz, M.I., Hunston, L.D. (1971). Biochemistry, 10, P 3065.
- Kong, J., Yu, S. h.(2007). Fourier Transform Infrared Spectroscopic Analysis of Protein Secondary Structures. Acta biochimica et Biophysica Sinica, 39(8), P 549-559.
- Krimm, S., Bandekar, J. (1986). Adv. Protein Chem., 38 , p181.
- Krishnakumar, S.S., Panda, D. (2002). Biochemistry,41, P7443.
- Lakowicz, J. R. (2006): Principles of Fluorescence Spectroscopy, 3rd ed, Springer Science Business Media, LLC .
- Levels of Protein Structure. http://www.biotopics.co.uk/JmolApplet/proteinjstructure.html
- Li, J., Ren, C., Zhang,Y., Liu, X., Yao, X., Hu., Z..(2008). Human serum albumin interaction with honokiol studied using optical spectroscopy and molecular modeling methods. Journal of Molecular Structure,881,P 90–96.
- Li, Y., He, W.Y., Liu, H., Yak, X., Hun, Z. (2007). Journal of Molecular Structure, 831, P 144.

- Li, Y., Ying, He, W., Ming, D., Shenga, F., Zhi, D (2006). Human serum albumin interaction with formononetin studied using fluorescence anisotropy, FT-IR spectroscopy, and molecular modeling methods .Bioorganic & Medicinal Chemistry,14,P 1431–1436.
- Liddell, H.G. & Scott, R. (1940). A Greek-English Lexicon. Revised and augmented throughout by Sir Henry Stuart Jones with the assistance of Roderick McKenzie. Oxford: Clarendon Pre
- Litwack. G, Axelord. J. (1970): Binding of Hormones to Serum Proteins. Biochemical Actions of Hormones. Volume.1. New York: Academic Press, INC. p 209-260.
- Matsuura, H., Hasegawa, K., Miyazawa, T. (1986). Spectrochim. Acta, 42, p1181.
- Mirabeela, F. M. (ED) (1998): Modern Techniques in Applied Molecular Spectroscopy, John Wiley & Sons Ltd, UK.
- NanoDop 3300 Fluorospectrometer V2.7 user's Manual, 2008, Thermo Fisher Scientific.
- NanoDrop 1000 Spectrophotometer V3.7, User's Manual, 2008, Thermo Fisher Scientific.
- Narhi, L. O. (2013): Biophysics for Therapeutic protein Development, 1st, Springer Science + Business media, USA.
- Nelson DL, Cox MM (2005). Lehninger's Principles of Biochemistry (4th ed.). New York, New York: W. H. Freeman and Company.
- Nikolić, G. S. (2011): Fourier Transforms - New Analytical Approaches and FT-IR Strategies, In Tech Janeza Trdine 9, 51000 Rijeka, Croatia.
- Norman, A.W., Mizwicki, M.T., Norman, D.P..(2004). Nature Reviews: Steroid-Hormones Rapid Actions, Membrane Receptors and a Conformational Ensemble model. Nature Reviews. Volume 3.
- OPUS bruker manual version 5.5, 2004 BRUKER OPTIK GmbH.
- Ouameur,A., Mangier,S., Diamantoglou, R., Rouillon, R., Carpentier H. A., Tajmir, R.. (2004). Effects of Organic and Inorganic Polyamine Cationson the Structure of Human Serum Albumin. Biopolymers, Vol. 73, 503–509
- Pace C, Shirley B, McNutt M, Gajiwala K (1 January 1996). "Forces contributing to the conformational stability of proteins". FASEB J. 10 (1): 75–83.
- Patel, S. K., Lavasanifar, A., Choi, P. (2010). Molecular Dynamics Study of the Encapsulation Capability of a PCL-PEO Based Block Copolymer for Hydrophobic Frugs with Different Spatial Distributions of Hydrogen Bond Donors and Acceptor. Biomaterials, 31, p 1780-1786.
- Pavia, D. L., Lampman, G. M., Kriz, G. S., Vyvyan, J. R (2009): Introduction to Spectroscopy, 4th, Brooks/Cole, Cengage learning, USA.
- Pearlman, H. W., Crepy. O.. (1967). The Journal of Biological Chemistry, Vol.242, No.2, p 182-189.
- Peng L., Minboa H., Fang C., Xi, L., Chaocan, Z. (2008). Protein $ Peptide Letters, 15, P360.

- Petitpas, I., Bhattacharya, A. A., Twine, S., East, M., Curry, S. (2001). Journal of Biological Chemistry, 276, P 22804.
- Prof. Subodh Kumar. (2006): Spectroscopy of Organic Compounds.
- Purcell, M., Neault J. F., Tajmir-Riahi, H. A. (200). Biochimica et Biophysica Acta, 1478, p61.
- Reece, J. B., Urry, A. L., Cain L. M., Wasserman, A.S., Minorsky V. P., Jackson, B. R.(2011): Campbell Biology. Pearson Benjamin Cummings, 9th ed. USA.
- Reed WL, Clark ME, Parker PG, Raouf S. A, Arguedas N, Monk D. S, Snajdr E, Nolan V, Ketterson ED (May 2006). "Physiological effects on demography: a long-term experimental study of testosterone's effects on fitness".
- Richardson, J.S.(2007): The Anatomy and Taxonomy of Protein Structure. DukeUniversity.http://kinemage.biochem.duke.edu/teaching/anatax/index.html
- Rondeau, P.A., Armenta S. B., Caillens, H. C., Chesne, S. A., Bourdon, E. A.(2007). Assessment of temperature effects on b-aggregation of native and glycated albumin by FT-IR spectroscopy and PAGE: Relations between structural changes and antioxidant properties. Archives of Biochemistry and Biophysics,460, P141–150.
- Rose G, Fleming P, Banana J, Martian A (2006). "A backbone-based theory of protein folding". Proc. Natl. Acad. Sci. U.S.A. 103 (45).
- Rosman, B. (2008). Calculation of Molecular Vibrational Normal Modes./www.homepages.inf.ed.ac.uk/
- Serdyuk, I. N., Zaccai, N. R., Zaccai, J. (2007): Methods in Molecular Biophysics Structure, Dynamics, Function, Cambridge University Press, New York.
- Settle, F.A (1997): Handbook of Instrumental Techniques for Analytical Chemistry, Infrared Spectroscopy, Prentice Hall PTR (ECS Professional).
- Shernan, M. (2014). Infrared Spectroscopy: A Key to Organic Structure, Yale-New Haven Teachers Institute.
- Soukpo´e-Kossi, C. N. N., Sedaghat-Herati, R. C., Hotchandani, S., Tajmir-Riahi, H. A (2007). International Journal of Biological Macromolecules, 40, p 484–490.
- Stephanos, J., Farina, S., Addison, A.(1996). Biochem.Biophys.Acta, 1295,p 209-221.
- Stephanos, J. J., Inorg J (1996). Biochem, 62, P155.
- Stuart B. (1997): Biological Applications of Infrared Spectroscopy,1st, John Wiley & Sons Ltd, UK.
- Surewicz, W.K., Mantsch, H.H., Chapman, D. (1993). Biochemistry,32, P 389.
- Tang, J., Luan, F., Chen, X. (2006) Molecular Modeling. Bioorg. Med. Chem.,14 pp. 3210–3217
- Testosterone.http://www.medicinenet.com/testosterone
- The Franklin Institute Inc. "Blood – The Human Heart". Retrieved 19 March 2009.

- The Space Science Laboratory, ES76 Biophysics, Marshall Space Flight Center, USA. Xiao-Min-He, Daniel C. Carter. Atomic Structure and Chemistry of Human Serum Albumin. Vol 358.16 July 1992.
- The Space Science Laboratory, ES76 Biophysics, Marshall Space Flight Center, USA. Daniel C. Carter, Xiao-MinHe, Sibyl H. Munson, Pamela D. Twigg, Kim M. Gernert, M. Beth Broom, Teresa Y. Miller. Three-Dimensional Structure of Human Serum. 9th June 1989.
- Thermo Nicolet (2001). Introduction to Fourier Transform Infrared Spectrometry, Thermo Nicolet Corporation, USA.
- Tian J. N., Liu, J. Q., Zhang, J. Y., Hu, Z. D., Chen, X G (2003). Chem. Pharm. Bull., 51, P 702.
- Tushar K. M., Kalyan S. G., Anirban S., Swagata D (2008). The interaction of silibinin with human serum albumin: A spectroscopic investigation. Journal of Photochemistry and Photobiology A: Chemistry 194 (297–307),
- Uversky, V. N., Permykov, A. E. (2007): Methods in Protein Structure and Stability Analysis; Vibrational spectroscopy, Nova Science Publishers, Inc, Hauppauge, New York.
- Venkataramana, G. V., KUMAR, J. K., PRASAD, A. G. D., Karimi, B (2010). Romanian J. Biophys, 20, p315–322
- Vij, D. R. (2006): Handbook of Applied Solid State Spectroscopy, Springer Science Business Media, LLC, USA.
- Wang, T., Xiang, B., Wang, Y., Chen, C., Dong, Y., Fang, H., Wang, M. (2008). Colloids Surf. B, 65, P113.
- Whitford, D. (2005): Proteins Structure and Function. England: John Wiley & Sons Ltd.
- Wilson, E. B., Decius, J. C., Cross, P. C..(1955): ‘‘Molecular Vibrations: The Theory of Infrared and Raman Vibrational Spectra’’, McGraw-Hill, New York.
- Workman, J. R. (1998): Applied Spectroscopy: Optical Spectrometers, Academic Press, San Diego.
- Wybranowski, T., Cyrankiewicz, M., Ziomkowska, B., Kruszewski, S.. (2008). (The HSA affinity of warfarin and flurbiprofen determined by fluorescence anisotropy measurements of camptothecin. BioSystems,94, P 258–262.
- Yamamoto, T., Tasumi, M. (1991). J. Mol. Struct., 242, p235.
- Yang, M.M., Yang, P., Zhang, L.W. (1994). Chin. Sci. Bu, 39, p734.
- Zhang G., Que Q., Pan J., Guo J (2008). Study of the interaction between icariin and human serum albumin by fluorescence spectroscopy. Journal of molecular structure 881, P 132-138.

ملخص

دراسة تأثير التستوستيرون على الالبومايين البروتين الناقل في بلازما الدم بواسطة تقنيات مطيافة الجزيئات

روان محمد خالد القواسمي.

إشراف: الدكتور موسى أبو طير والأستاذ الدكتور محمود أبو حديد

تم دراسة التفاعل بين البروتين الناقل في بلازما الدم (الالبومايين) و هرمون التستوستيرون باستخدام مطياف الأشعة فوق البنفسجية (UV-vis spectrophotometer) و جهاز انبعاث الإشعاع (Fluorescence spectrophotometer) ومطياف تحويل فوريير للأشعة تحت الحمراء (Fourier transform infrared spectroscopy). في هذه التجربة تم حساب ثابت الترابط (binding constant) للتستوستيرون و الالبومايين الناقل عن طريق مطياف الأشعة فوق البنفسجية ومطياف انبعاث الإشعاع و القيمة هي: $34.9\times10^{2}\ M^{-1}$ تحليل طيف الانبعاث أوصل إلى حساب ثابت الترابط للتفاعل لتكون القيمة $\times10^{2}\ M^{-}$ 38.23^{1}، مما يشير إلى نتائج متقاربة لثابت الترابط بطرق الحساب المختلفة. بمقارنة ثابت تفاعل التستوستيرون و الالبومايين مع تفاعل البروجستيرون و الكولسترول مع الالبومايين نستخلص ان ترابط التستوستيرون مع الالبومايين هو الأقوى لوجود مستقبل ومتطوع للرابطة الهيدروجينية في التركيب الكيميائي للتستوستيرون.

وتم حساب ثابت (Stern-Volmer constant) وثابت (quenching rate) للترابط بين التستوستيرون و الالبومايين و القيم هي: ($4.5\times10^{2}\ L\ Mol^{-1}$، $4.5\times10^{10}\ L\ Mol^{-1}$) على التوالي. ومن نتائج الدراسة أن شدة امتصاص الأشعة فوق البنفسجية للالبومايين تزداد بزيادة تركيز التستوستيرون عند ثبات تركيز الالبومايين. و من خلال استخدام جهاز انبعاث الإشعاع وجد ان شدة الإشعاع المنبعث نتيجة تفاعل التستوستيرون مع الالبومايين تقل بزيادة تركيز التستوستيرون وثبات تركيز الالبومايين.

وقد تم استخدام مطياف تحويل فوريير للأشعة الحمراء (FT-IR) مع تطبيق عدد من التقنيات الموجودة مثل (Fourier Self Deconvolution) و (Resolution Second Derivative) بالإضافة إلى (Curve Fitting) لتحليل مناطق الأميد الأول والثاني والثالث لهرمون التستوستيرون من أجل تحديد بنية البروتين الثانوية (Secondary Structure) و آلية ارتباط التستوستيرون مع الالبومايين. تحليل قياسات جهاز FT-IR تشير إلى ان زيادة تركيز التستوستيرون تقود إلى (protein unfolding) ونقص في نسبة حزم الامتصاص التابعة ل α-helical structure مقابل زيادة نسبة حزم الامتصاص التابعة ل β sheet structure

تمثل هذه النتائج أهمية أساسية في مجال تصميم الأدوية، وإعطاء معلومات عن حدوث تغييرات على هيكل الالبومايين بسبب تفاعله مع هرمون التستوستيرون، فوق المساعدة في أعمال التشخيص في حالة اضطراب تركيز هرمون التستوستيرون بغض النظر عن مصدره الطبيعي أو المنشط و كيف يؤثر ذلك على بنية البروتين. فدراسة تفاعل التستوستيرون مع الالبومايين لتلك الحالات يساعد في التنبؤ بوجود حالات اضطراب الهرمون بمقارنة حالات التركيز العادية و العالية. و ويمكن لقابلية الالبومايين الارتباط بالجزيئات و العقاقير الأخرى ان تتأثر بسبب استعداده المتزايد للارتباط بالتستوستيرون مما يمكن أن يؤدي إلى نقص في تراكيز هذه المواد داخل الأنسجة المستهدفة بسبب إحتمالية ارتباط الالبومايين بالتستوستيرون.

ينصح بمزيد من التحقيقات في مجال تأثير درجة الحرارة على تفاعل التستوستيرون مع الالبومايين وكيف سوف يتغير هيكل البروتين مع تغير درجة الحرارة.